

A MINIATURIZED INTERDIGITAL HAIRPIN MICROSTRIP BANDPASS FILTER DESIGN

**A dissertation submitted in partial fulfillment of requirement for the degree of Bachelor of
Science in Electrical and Electronic Engineering**

ISLAMIC UNIVERSITY OF TECHNOLOGY

The Organization of the Islamic Cooperation (OIC)



SUBMITTED BY

Nafiul Islam

Istiaque Islam

Md. Merazul Haque

UNDER THE SUPERVISION OF

DR. MD. FOKHRUL ISLAM

ASSISTANT PROFESSOR

DEPARTMENT OF ELECTRICAL AND ELECTRONIC ENGINEERING

ISLAMIC UNIVERSITY OF TECHNOLOGY, BANGLADESH.

A MINIATURIZED INTERDIGITAL HAIRPIN MICROSTRIP BANDPASS FILTER DESIGN

**A Thesis Presented to
The Academic Faculty**

By

Nafiul Islam (Student ID : 082407)

Istiaque Islam (Student ID : 082424)

Md. Merazul Haque (Student ID : 082456)

**In Partial Fulfillment of Requirement for the Degree of Bachelor of Science in
Electrical and Electronic Engineering**

ISLAMIC UNIVERSITY OF TECHNOLOGY

October, 2012

**A MINIATURIZED INTERDIGITAL HAIRPIN
MICROSTRIP BANDPASS FILTER DESIGN**

Approved By :

DR. MD. FOKHRUL ISLAM

ASSISTANT PROFESSOR

DEPARTMENT OF ELECTRICAL AND ELECTRONIC ENGINEERING

ISLAMIC UNIVERSITY OF TECHNOLOGY, BANGLADESH

The Thesis titled

A MINIATURIZED INTERDIGITAL HAIRPIN MICROSTRIP BANDPASS FILTER DESIGN

Submitted by Nafiul Islam (Std. No. 082407), Istiaque Islam (Std. No. 082424), Md. Merazul Haque (Std. No. 082456) of Academic year 2011-2012 has been found as satisfactory and accepted as partial fulfillment of the requirement for the Degree Bachelor of Science in Electrical and Electronic Engineering.

Prof. Dr. Md. Shahid Ullah

Professor

Head of the Department

Department of EEE

Islamic University of Technology

Dr. Md. Fokhrul Islam

Assistant Professor

Supervisor

Department of EEE

Islamic University of Technology

Project Members:

Nafiul Islam

Istiaque Islam

Md. Merazul Haque

Declaration of Candidates

It is here by declared that this thesis or any part of it has not been submitted elsewhere for the award of any Degree or Diploma.

Dr. Md. Fokhrul Islam, Supervisor

Assistant Professor

Department of EEE

Islamic University of Technology

Nafiul Islam

(Student ID: 082407)

Istiaque Islam

(Student ID: 082424)

Md. Merazul Haque

(Student ID: 082456)

CONTENTS

	Page
LIST OF FIGURES	vi
LIST OF TABLES	viii
LIST OF SYMBOLS AND ABBREVIATIONS	viii
ACKNOWLEDGEMENTS	ix
ABSTRACT	x
<u>CHAPTER</u>	
1. INTRODUCTION	
1.1 Basic of wireless communication	1
1.2 Microstrip band-pass filter	2
1.3 Contribution of the thesis	3
1.4 Organization of the thesis	3
2. BACKGROUND	
2.1 Band-pass filter	4
2.2 Properties of band-pass filter	5
2.3 Filter transmission	8
2.4 Design techniques of band-pass filter	9
2.5 Literature review	10
3. PROPOSED FILTER	
3.1 Specifications	15
3.2 Optimization	16
4. RESULTS AND SIMULATIONS	
4.1 Simulated result	19
4.2 Comparison between models	20
4.3 Insight into parametric study	20
5. CONCLUSION	22
APPENDIX A:	23
APPENDIX B:	27
REFERENCES	42

List of Figures

	Page
Figure 1.1: Ideal transmission characteristics of four types of filters	1
Figure 1.2: Hairpin Resonator	2
Figure 2.1.1: System level block diagram of a band-pass filter	4
Figure 2.1.2 (a): A medium-complexity example of a band-Pass filter	4
Figure 2.1.2 (b): Transfer function versus frequency for a band-pass filter	5
Figure 2.2.1: Magnitude transfer function of a bandpass filter	6
Figure 2.2.2: Passband Signal	6
Figure 2.2.4: Insertion and Return Loss	7
Figure 2.3: Two-port network	9
Figure 2.5.2 (a): Interdigital Hairpin Resonator	11
Figure 2.5.2 (b): Layout of the microstrip four pole elliptic function compact filter	11
Figure 2.5.3 (a): Simulated Frequency response for FR4 Substrate	13
Figure 2.5.3 (b): Measured Frequency response for FR4 Substrate	13
Figure 3.1: Interdigital hairpin resonator	16
Figure 3.2: Frequency response with $I_{dd}=1$ mm	17
Figure 3.3: Frequency response with $I_{dd}=0.5$ mm	17
Figure 3.4: Frequency response with $I_{dd}=0.95$ mm	18
Figure 3.5: Layout of the microstrip four-pole elliptic function compact filter	18
Figure 4.1: Frequency response of the proposed model	19
Figure B1: Zeland Program Manager	27
Figure B2: Main view of MGRID	28
Figure B3: Basic parameter definitions	28
Figure B4: Defining the parameters of the filter substrate	29
Figure B5: Layout view of the problem after the definition of the dielectric layers	29

Figure B6: Rectangle pop-up window	30
Figure B7: Mgrid window	30
Figure B8: Keyboard input absolute location pop-up window	31
Figure B9: Keyboard input relative location pop-up window	31
Figure B10: Mgrid window	32
Figure B11: Mgrid window	32
Figure B12: Mgrid window	33
Figure B13: Mgrid window	33
Figure B14: Mgrid window	34
Figure B15: Mgrid window	34
Figure B16: Mgrid window	35
Figure B17: Mgrid window	35
Figure B18: Mgrid window	36
Figure B19: Mgrid window	36
Figure B20: Mgrid window	37
Figure B21: Modua window	37
Figure B22: Mgrid window	38
Figure B23: Mgrid window	38
Figure B24: Mgrid window	39
Figure B25: Automatic meshing parameter pop-up window	39
Figure B26: Mgrid window	40
Figure B27: Simulation setup pop-up window	40
Figure B28: Frequency response in Modua	41

List of Tables

	Page
Table 4.1: Comparison between existing model and proposed model	20
Table 4.2: Parametric (Idd) study	21
Table A1: RO4000® Series Laminate Product Information	25
Table A2: RO4000 Series Materials Dielectric Constant vs. Temperature	26
Table A3: RO4000 Series Materials Dielectric Constant vs. Frequency	26
Table A4: Microstrip Insertion Loss (0.030" Dielectric Thickness)	26

List of Symbols and Abbreviations

ϵ_r	Dielectric Constant
GHz	Giga Hertz
IEEE	Institute of Electrical and Electronic Engineers
IE3D	Moment of Method Based EM Simulator
BW	Bandwidth
RL	Return Loss
IL	Insertion Loss
Q	Quality Factor
fr	Resonant Frequency
PBW	Percentage Bandwidth
M_{ij}	Coupling Coefficient
C	Lump Capacitance
j	Characteristics Admittance
f_0	Center Frequency
Idd	Interdigital distance
FBW	Fractional band width

ACKNOWLEDGEMENT

We would like to thank our supervisor **Dr. Md. Fokhrul Islam** for his many directions, suggestions and corrections. Without his guidance, we do not believe this thesis would have been completed. We would like to express our heartiest gratitude to him for his great support for helping us understand the basics and building the hardware for acquisition of the project. We express our thankfulness to **Prof. Dr. Md. Shahid Ullah**, head of the Department of Electrical and Electronic Engineering for providing us with best facilities in the department and his timely suggestions.

Last but not least we would like to thank all of our friends who were involved directly or indirectly in successful completion of the present work.

- Nafiul Islam
- Istiaque Islam
- Md. Merazul Haque

ABSTRACT

Modern communication technology is advancing every day. It is becoming more efficient and miniaturized. The efficiency of the communication technology depends upon the performance of the filter used in the system. That's why extensive research is going on to improve the filter performance as well as to reduce its size.

In this thesis we have proposed a four-pole elliptic function band-pass filter designed using compact miniaturized microstrip interdigital hairpin resonator. Miniaturization hairpin resonator is realized by using an interdigital structure having parallel coupled lines.

Many works are going on in the field of filter designing. The most recent works has been studied in this thesis to obtain the most suitable design for specific application. We have used the full-wave simulator IE3D to design the interdigital hairpin resonator.

We choose RO4003C substrate for our design as it has many advantages in high frequency applications.

Finally a filter with chip area of $28.2 * 20.2 \text{ mm}^2$ and center frequency at 2.4GHz with a 3db bandwidth of 220 MHz has been proposed. Its upper cutoff and lower cutoff frequencies are respectively 2.53 GHz and 2.31 GHz.

CHAPTER 1 INTRODUCTION

1.1 Basics of wireless communication

Antenna and filter are two most important parts of wireless communication. An antenna converts the electrical energy into wave energy or vice versa and a filter selects frequency at which the system will operate.

A filter is a circuit which is designed to pass a specific band of frequencies while attenuating all signals outside this band. Filter network can be either active or passive. Passive filter networks only resistors, inductors and capacitor. Passive filters are good for high frequency applications but for low frequency applications large inductors are needed causing a bulky system which is often discouraged. Active filters employ transistors or op-amps plus resistors, inductors and capacitors. The use of inductors in the active filter is often discouraged as they are bulky, costly and they may have large internal resistive components.

There are four types of filters: low-pass, high-pass, band-pass and band reject filters.

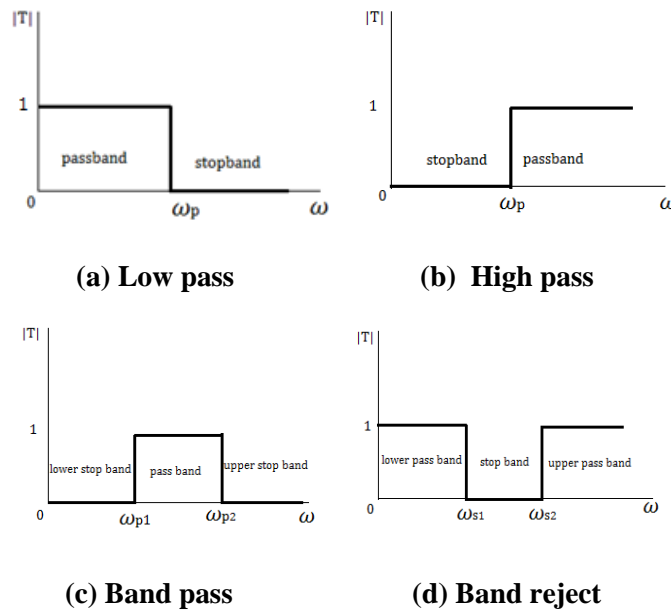


Fig 1.1: Ideal transmission characteristics of four types of filters (a) low pass (b) high pass (c) Band pass (d) Band reject

Figure: 1-1 illustrates the frequency response plots for four kinds of filters. A low-pass filter circuit has a constant output voltage from dc up to a cut-off frequency f_c . As the frequency increases beyond f_c the output voltage is attenuated (decreased). Figure:1.1(a) shows the magnitude of the output voltage of a low-pass filter. The ranges of frequencies that are transmitted are called pass-band and the ranges of

frequencies that are attenuated are called stop-band. The cut-off frequency is also known as .707 frequency, - 3dB frequency, or the break frequency.

High-pass filters attenuate the output voltage for all frequencies below the cut-off frequency f_c . Above f_c the magnitude of the output voltage is constant.

Band-pass filters only pass a band of frequencies while attenuating all frequencies outside the band. Band-reject filters works in exactly opposite way. Band-reject filters reject a specified band of frequencies while passing all the others.

1.2 Microstrip band-pass filter

In recent years, the trend in communication system has been to develop low cost, minimal dimension filter which are capable of high performance. Miniaturization of filter makes a circuit compact with high performance and that's why microstrip filter are being introduced.

With modern day printed circuit board technology it has become a common practice to use microstrip band-pass filters. There are several microstrip structures: Parallel coupled line, Split ring resonators, Hairpin resonators. And some further improvement in hairpin resonators is interdigital hairpain resonator.



Fig 1.2: (a) Conventional hairpin resonators (b) Miniaturized hairpin resonators using coupled lines (c) Inter digital hairpin resonators.

Our primary objective is to find out a suitable design of microstrip band-pass filter using interdigital hairpin resonator and reduce its dimension. Many designs are available for various applications which is covered in the literature review portion. Once we have developed a suitable design we have to choose a substrate with low die-electric loss, low Z-axis expansion and good performance at high frequency.

Then the band-pass filter is designed using IE3D simulation software. IE3D is a general purpose electromagnetic simulation and optimization package that has been developed for design and analysis of planner and 3D structures encountered in microwave and MMIC, high temperature superconductor (HTS) circuits, microstrip antennas, microstrip filters, Radio frequency (RF) printed circuit board (PCB) and high speed digital circuit packaging. Based upon an integral equation, method of moment (MoM)

algorithm, the simulator can accurately and efficiently simulate arbitrarily shaped and oriented 3D metallic structures in multi-layer die-electric substrate. With this software we can easily design our filter and simulate the results and also point out the effect of various parameters and thus select the most efficient model.

1.3 Contribution of the thesis

A band-pass filter with center frequency of 2.4 GHz and bandwidth of 220 MHz has been designed which can be used specially in personal communication system (PCS) and other microwave application. The dimension of the band-pass filter is $(28.2*20.2)$ mm² which is the most compact design for microwave application (1-4 GHz) available right now.

1.4 Organization of the thesis

The dissertation is mainly divided into five chapters.

Introduction to basic wireless communication, microstrip band-pass filter, interdigital hairpin resonator and main objectives of the thesis have already been expressed in chapter 1.

Chapter 2 provides some information about basic properties of filter and the literature review done in the process.

Based on the literature review a filter is taken for optimization. Optimization is done by simulating the filter with variable parameters. The effects of this parametric study and the final optimized design are discussed in chapter 3.

The final output characteristics and the comparison with existing filters and proposed filter is briefly discussed in chapter 4. Also the effects of parametric study have been summarized to understand the effect of different parameters on bandwidth, resonance, idd and return loss.

Finally conclusive discussions and scope for future works are described in the fifth and the final episode.

CHAPTER 2 BACKGROUND

2.1 Band-Pass Filter

2.1.1 Definition

A band-pass filter is a device that passes frequencies within a certain range and rejects (attenuates) frequencies outside that range. Band-pass is an adjective that describes a type of filter or filtering process; it is frequently confused with passband which refers to the actual portion of affected spectrum. Hence, one might say "A dual band-pass filter has two passbands." A band-pass signal is a signal containing a band of frequencies away from zero frequency, such as a signal that comes out of a band-pass filter.

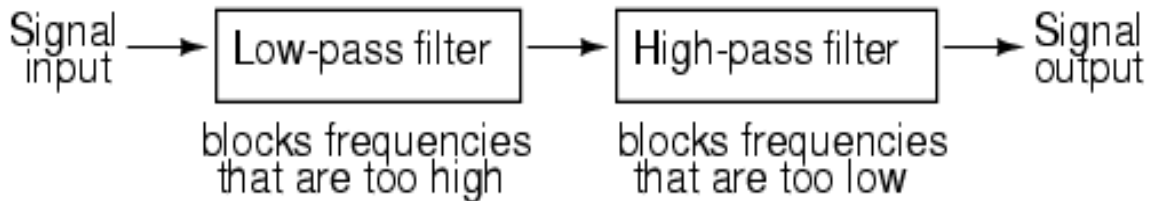


Figure 2.1.1: System level block diagram of a band-pass filter

2.1.2 Characteristics of Band-pass Filter

An ideal bandpass filter would have a completely flat passband (e.g. with no gain/attenuation throughout) and would completely attenuate all frequencies outside the passband. Additionally, the transition out of the passband would be instantaneous in frequency. In practice, no bandpass filter is ideal. The filter does not attenuate all frequencies outside the desired frequency range completely; in particular, there is a region just outside the intended passband where frequencies are attenuated, but not rejected. This is known as the filter roll-off, and it is usually expressed in dB of attenuation per octave or decade of frequency. Generally, the design of a filter seeks to make the roll-off as narrow as possible, thus allowing the filter to perform as close as possible to its intended design. Often, this is achieved at the expense of pass-band or stop-band ripple.

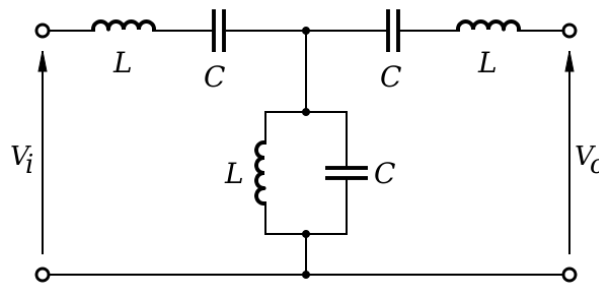


Figure 2.1.2 (a) : A medium-complexity example of a band-Pass filter

The bandwidth of the filter is simply the difference between the upper and lower cutoff frequencies. The shape factor is the ratio of bandwidths measured using two different attenuation values to determine the cutoff frequency, e.g., a shape factor of 2:1 at 30/3 dB means the bandwidth measured between frequencies at 30 dB attenuation is twice that measured between frequencies at 3 dB attenuation.

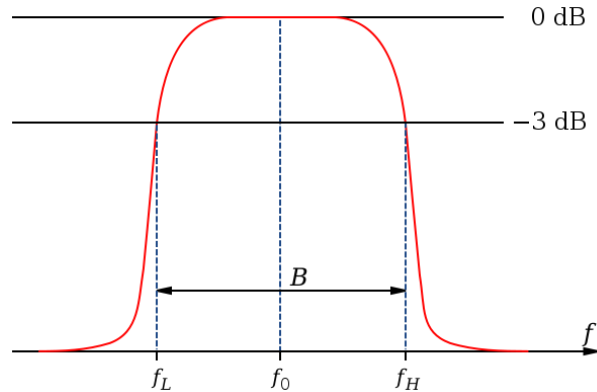


Figure 2.1.2 (b) : Bandwidth measured at half-power points (gain -3 dB, $\sqrt{2}/2$, or about 0.707 relative to peak) on a diagram showing magnitude transfer function versus frequency for a band-pass filter

2.2 Properties of Band-pass Filter

There are applications where a particular band, or spread, or frequencies need to be filtered from a wider range of mixed signals. Filter circuits can be designed to accomplish this task by combining the properties of low-pass and high-pass into a single filter. The properties of Band-pass filter are :

- **Upper Cutoff Frequency**
- **Lower Cutoff Frequency**
- **Passband**
- **Bandwidth**
- **Return Loss**
- **Insertion Loss**
- **Quality Factor**
- **S-parameters**

2.2.1 Cut-off Frequency: Upper and Lower Cut-off Frequencies

A **cutoff frequency**, **corner frequency**, or **break frequency** is a boundary in a system's frequency response at which energy flowing through the system begins to be reduced (attenuated or reflected) rather than passing through. There are two types of cut-off frequencies.

- Upper cut-off frequency
- Lower cut-off frequency

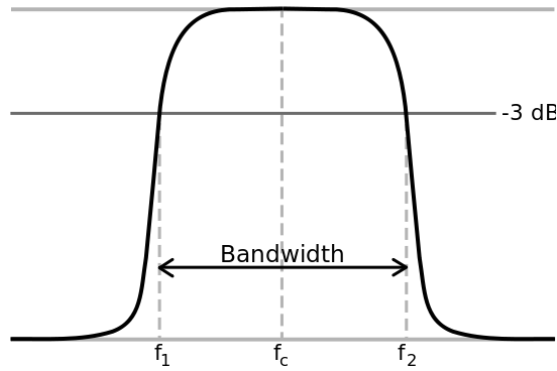


Figure 2.2.1: Magnitude transfer function of a bandpass filter with lower 3 dB cutoff frequency f_1 and upper 3dB cutoff frequency f_2

2.2.2 Passband

A **passband** (not to be confused with band-pass) is the portion of the frequency spectrum that is transmitted (with minimum relative loss or maximum relative gain) by some filtering device. In other words, it is a *band* of frequencies which *passes* through some filter or set of filters. The accompanying figure shows a schematic of a waveform being filtered by a bandpass filter consisting of a highpass and a lowpass filter.

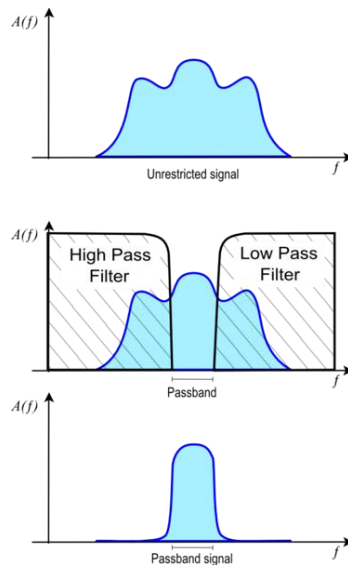


Figure 2.2.2: Unrestricted signal (upper diagram). Bandpass filter applied to signal (middle diagram). Resulting bandpass signal (bottom diagram). $A(f)$ is the frequency function of the signal or filter in arbitrary units.

2.2.3 Return loss

Return loss is the loss of signal power resulting from the reflection caused at a discontinuity in a transmission line or optical fiber. This discontinuity can be a mismatch with the terminating load or with a device inserted in the line. It is usually expressed as a ratio in decibels (dB).

$$RL(dB) = 10 \log_{10} \frac{P_i}{P_r}$$

where $RL(dB)$ is the return loss in dB, P_i is the incident power and P_r is the reflected power.

A filter performance characteristic providing the relative amount of power reflected by an input signal. In a perfect transmission line, there is no reflected power so Return Loss is essentially infinite. In a perfectly reflective circuit, Return Loss is zero.

2.2.4 Insertion loss

Insertion loss is the loss of signal power resulting from the insertion of a device in a transmission line or optical fiber and is usually expressed in decibels (dB).

If the power transmitted to the load before insertion is P_T and the power received by the load after insertion is P_R , then the insertion loss in dB is given by,

$$IL(dB) = 10 \log_{10} \frac{P_T}{P_R}$$

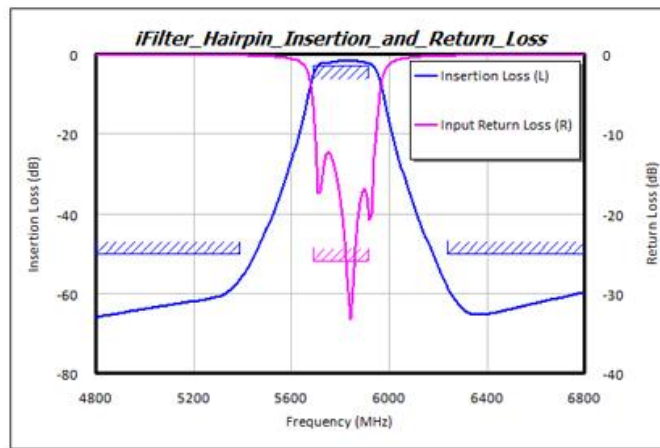


Figure 2.2.4 : Insertion and Return Loss

2.2.5 Quality Factor

A band-pass filter can be characterized by its **Q-factor**. A high-Q filter will have a narrow pass band and a low-Q filter will have a wide pass band. These are respectively referred to as narrow-band and wide-band filters. The Q factor is a dimensionless parameter that describes how under damped a resonator is or equivalently, characterizes a resonator's bandwidth relative to its center frequency. Higher Q indicates a lower rate of energy loss relative to the stored energy of the oscillator, i.e. the oscillations die out more slowly.

$$Q = \frac{f_0}{BW}$$

2.2.6 S-Parameters

Scattering parameters or **S-parameters** (the elements of a **scattering matrix** or **S-matrix**) describe the electrical behavior of linear electrical networks when undergoing various steady state stimuli by electrical signals.

S11 - Power reflected back to Port 1 from Port 1 (Port 1 Return Loss)

S22 - Power reflected back to Port 2 from Port 2 (Port 2 Return Loss)

S21 - Power loss through device from Port 1 to Port 2 (Insertion Loss)

S12 - Power loss through device from Port 2 to Port 1 (Insertion Loss)

Details discussed in appendix A

2.3 Filter Transmission

The filter we are about to study are linear circuits that can be represented by the general two-port network shown in Fig. 2.3. The filter transfer function $T(s)$ is the ratio of the output voltage $V_o(s)$ to the input voltage $V_i(s)$.

$$T(s) \equiv \frac{V_o(s)}{V_i(s)}$$

The filter transmission is found by evaluating $T(s)$ for physical frequencies, $s = j\omega$, and can be expressed in terms of its magnitude and phase as

$$T(j\omega) = |T(j\omega)|e^{j\varphi(\omega)}$$

The magnitude of transmission is often expressed in decibels in terms of the gain function

$$G(\omega) \equiv 20 \log |T(j\omega)|, \text{ dB}$$

Or, alternatively, in terms of the attenuation function

$$A(\omega) \equiv -20 \log |T(j\omega)|, \text{ dB}$$

A filter shapes the frequency spectrum of the input signal, $|V_i(j\omega)|$, according to the magnitude of the transfer function $|T(j\omega)|$, thus providing an output $V_o(j\omega)$ with a spectrum

$$|V_o(j\omega)| = |T(j\omega)||V_i(j\omega)|$$

Also, the phase characteristics of the signal are modified as it passes through the filter according to the filter phase function $\varphi(\omega)$.

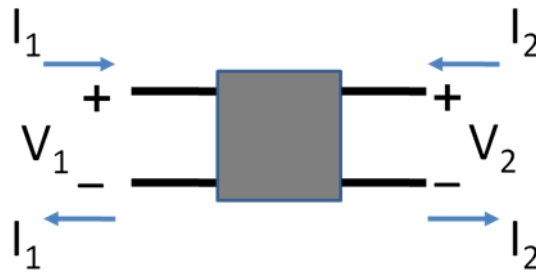


Figure 2.3 : The filters studied in this section are linear circuits represented by the general two-port network shown.

$$\text{The filter transfer function } T(s) \equiv \frac{V_o(s)}{V_i(s)}$$

2.4 Design Techniques of Band-pass Filter

2.4.1 Photonic Band Gap (PBG)

- A periodic structure designed to reject a particular band gap.
- Due to radiation from the periodic etched defects cannot be used to design microwave component.

2.4.2 Ground Plane Aperture (GPA)

- Under micro strip line ,line properties could be changed due to variation of characteristics impedance with the width of GPA.

2.4.3 Defected Ground Structures(DGS)

- It overcomes the problems discussed above.
- The selectivity of a filter improves.

But among these design techniques the DGS is the most preferred techniques. Many people have presented numerous design techniques regarding DGS:

2.4.3.1 Parallel coupled line :

- Suffers from spurious response which degrades the pass band and stop band performance.
- size of the filter designed is quite large and has limited selectivity.

2.4.3.2 Split ring resonators :

- suffer from large resonance frequency variation and large circuit losses.

2.4.3.3 Hairpin resonators :

- Overcome above disadvantages.
- Compact size and low cost.

2.5 Literature Review

2.5.1

In wireless communication systems, small size and high performance filters are needed to reduce the cost and improve the system performance. They can be designed in many different ways. However, further miniaturization becomes more difficult for this filter. Planar filters provide good miniaturization ability [1– 4]. Therefore, there has been much research conducted on planar filters and their components. Since microstrip resonators are the basic components of a planar filter design, it is necessary to select proper resonator types used in a filter design. A conventional half-wavelength open-line microstrip resonator is too large to be used in the modern communication system such as 900 MHz, 1800 MHz for personal communication systems (PCS). The hairpin filters [1, 5–7] were folded from the open line $\frac{\lambda}{2}$ wavelength microstrip resonator to become U-shaped resonators and make progress in circuit size reduction from the parallel-coupled line structure. Since 1989, the miniaturized hairpin resonator was developed by several researchers [7–9]. The interdigital coupled lines at the ends of this structure are used as a capacitor to reduce the resonator size. In addition, cross-coupled filter with these attractive characteristics is that of quasi-elliptic function response filters with a pair of attenuation poles at finite frequencies [10, 11]. The capability of placing attenuation poles near the cutoff frequencies of the pass-band improves the selectivity using less resonators. A cross-coupled between a pair of nonadjacent resonators approached this type filter. The filter employing the cross coupled generally results in a compact topology. In this article, a design of a microstrip four-pole cross-coupled elliptic function filter using compact interdigital hairpin resonators was presented. The design approach enables one to use EM simulator to complete the filter design, to determine the physical dimensions of the filters.

2.5.2 Interdigital Hairpin Filter Design

Figure 2.5.2(a) shows the layout and equivalent electrical parameters of an interdigital hairpin resonator. Its fundamental condition is hence the same as that of a conventional miniaturized hairpin resonator [12]. In the case of $Z_s > \sqrt{Z_{i0}Z_{ie}}$, the total electrical length of these resonators becomes shorter than that of conventional. Further miniaturization can be achieved by increasing the coupling between parallel coupled lines and hence decreasing the value of $\sqrt{Z_{i0}Z_{ie}}$. In addition, the resonance condition can be calculated from input admittance using ABCD matrices [13]. The dimensions of miniaturized resonator with a center frequency of 1.8 GHz are shown in Figure 2.5.2(a).

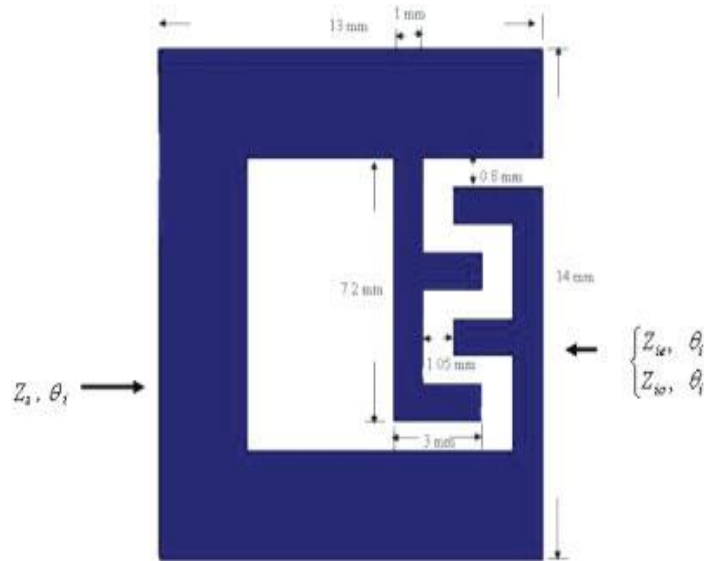


Figure 2.5.2(a): Interdigital Hairpin Resonator

A four-pole elliptical bandpass filter response can be implemented using the cross coupling between nonadjacent resonators. The cross-couplings give the input signal two paths from the input port to the output. The magnitude and phase of the signal are changed differently through different paths. As mentioned above, the multipath effect may cause attenuation poles at finite frequencies if the couplings among the resonators are properly designed. Figure 2.5.2(b) shows the four-pole elliptic function bandpass filter with using miniaturized hairpin resonators. In the configuration, significant couplings exist between any two nondiagonally neighboring miniaturized hairpin resonators. The structure can be extended to form cross-coupled filters of higher orders.

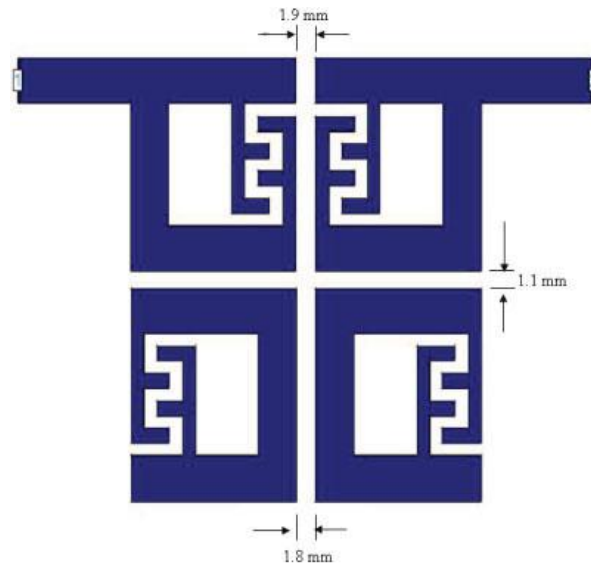


Figure 2.5.2(b) : Layout of the microstrip four pole elliptic function compact filter

Cross-coupled bandpass filters with using compact hairpin resonators are designed to have a fractional bandwidth of 5% at a mid-band frequency $f_0 = 1.8$ GHz. The filter was fabricated on FR4 substrate. A

four-pole (n=4) Elliptic function low-pass prototype with a Ω_a value of 1.85 is chosen. The lumped circuit element value with $\Omega_a = 1.85$ of low-pass prototype filter are found to be $C_1=0.95826$, $C_2=1.40972$, $J_1=0.19685$, and $J_2=1.10048$. The relationships between the band-pass design parameters and the low-pass elements are as follows [14]:

$$\begin{aligned}
 Q &= \frac{C}{\text{FBW}} = 19.1652 \\
 M_{12} &= M_{34} = \frac{\text{FBW}}{\sqrt{(c_1 c_2)}} = 0.043 \\
 M_{14} &= \frac{\text{FBW} \times j_1}{c_1} = -0.01 \\
 M_{23} &= \frac{\text{FBW} \times j_2}{c_2} = 0.039
 \end{aligned}$$

where, FBW denotes the fractional bandwidth of the band-pass filter, C is the capacitance of the lumped capacitor, and J is the characteristic admittance of the inverter, and N is the degree of the filter. The cross-coupled structure provides electric, magnetic, and mixed coupling. Using a parameter-extraction technique, we carry out EM-simulations to extract the external Q and coupling co-efficient M against the physical dimensions. The coupling co-efficient M_{ij} of each pair of coupled resonators can be calculated by using the equation as follows :

$$M_{ij} = \frac{(f_2^2 - f_1^2)}{(f_2^2 + f_1^2)} \dots\dots\dots (1)$$

where, f_1 and f_2 are the lower and higher split resonant frequencies. Therefore, the design curves for these coupling structures can be presented and shown in Figure 2.5.2(a). Figure 2.5.2(b) shows the feed location topology used in this filter design. The external Q of such feed structure can be characterized by the following:

$$Q = \frac{f_0}{\Delta f_{3\text{dB}}} \dots\dots\dots (2)$$

where, f_0 is the resonant frequency of the resonator and $\Delta f_{3\text{dB}}$ is the 3 dB bandwidth. The design curve of the feed location on the resonator for a given external Q can be obtained by using EM simulation tool such as IE3D [15]. By using the design curves of the coupling co-efficient and the external Q, this filter can be realized.

2.5.3 Results

Figure 2.5.3(a) shows calculated filter response of the cross-coupled compact interdigital hairpin filter with FR4 substrate. The simulation result of filter performance of the cross-coupled filter with 5.4%, the mid-band insertion loss 1.8 GHz. The bandwidth of each filters quite agree with the desirable values.

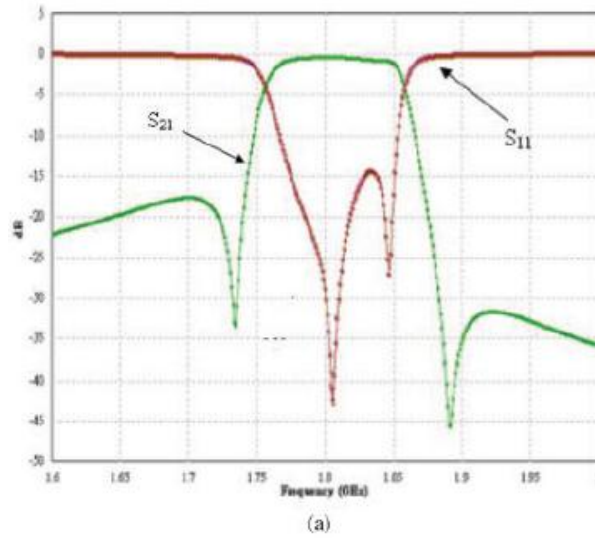


Fig 2.5.3(a) : Simulated Frequency response for FR4 Substrate

It was found that the sharper skirt properties of the cross-coupled filter. The measurements are performed with an HP8757D network analyzer. The measured performance is shown in Figure 2.5.3(b). With using FR4 substrate, the mid-band insertion loss is about 1.26 dB and the return loss is about 21 dB at the center frequency of 1.8 GHz, and 3 dB passband width is about 4.5%.

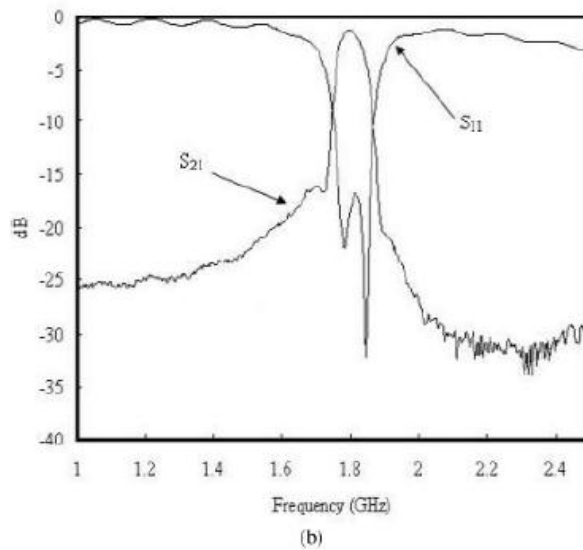


Fig 2.5.3(b) : Measured Frequency response for FR4 Substrate

A comparison between the measurement and simulation is presented that the measured response strongly influenced by fabricated processing.

2.5.4 Limitations of this design

After studying this design we have found several limitations:

- Dimension = 27.9 mm * 29.1 mm
- Thickness : 1.8 mm
- Disadvantages of FR4 substrate
 - I. dielectric losses in FR4 are too high at microwave frequencies.
 - II. the dielectric constant is not sufficiently tightly controlled.
 - III. FR4 is not suitable for circuitry near 2 GHz .
- Fractional BW at mid band = 5%
- dB BW = 100 MHz

CHAPTER 3

Proposed Filter

3.1 Specifications

Our primary objective is to design a more compact and efficient filter with high selectivity. Specifications of our proposed filter model are:

3.1.1 Dimension

We have proposed a filter having the area of $28.2 \times 20.2 \text{ mm}^2$. So it is more compact than the existing model.

3.1.2 Frequency range

The band pass filter will have the pass band within 2.31- 2.53 GHz.

3.1.3 Z-plan

Z plan means the thickness of the substrate used. The thickness will be 1.5 mm.

3.1.4 Dielectric constant

Dielectric constant of the substrate is 3.3.

3.1.5 Tangential loss

Tangential loss is 0.0021.

3.1.6 Substrate

We have chosen RO4003C as substrate. RO4003C laminates are designed to offer superior high frequency performance and low cost circuit fabrication. The result is a low loss material which can be fabricated using standard epoxy/glass (FR4) processes offered at competitive prices. This substrate has

- Non-PTFE-thermoset resin system
- High frequency performance due to low dielectric tolerance and loss.
- Stable electrical property vs. frequency
- Low thermal coefficient of dielectric constant
- Low Z-axis expansion
- Low in-plan expansion coefficient
- Excellent dimensional stability
- Volume manufacturing process

3.2 Optimization

After some intensive simulation we have obtained an optimized structure fulfilling our specification. As we have designed a four pole elliptical filter specifying only one interdigital hairpin resonator is enough.

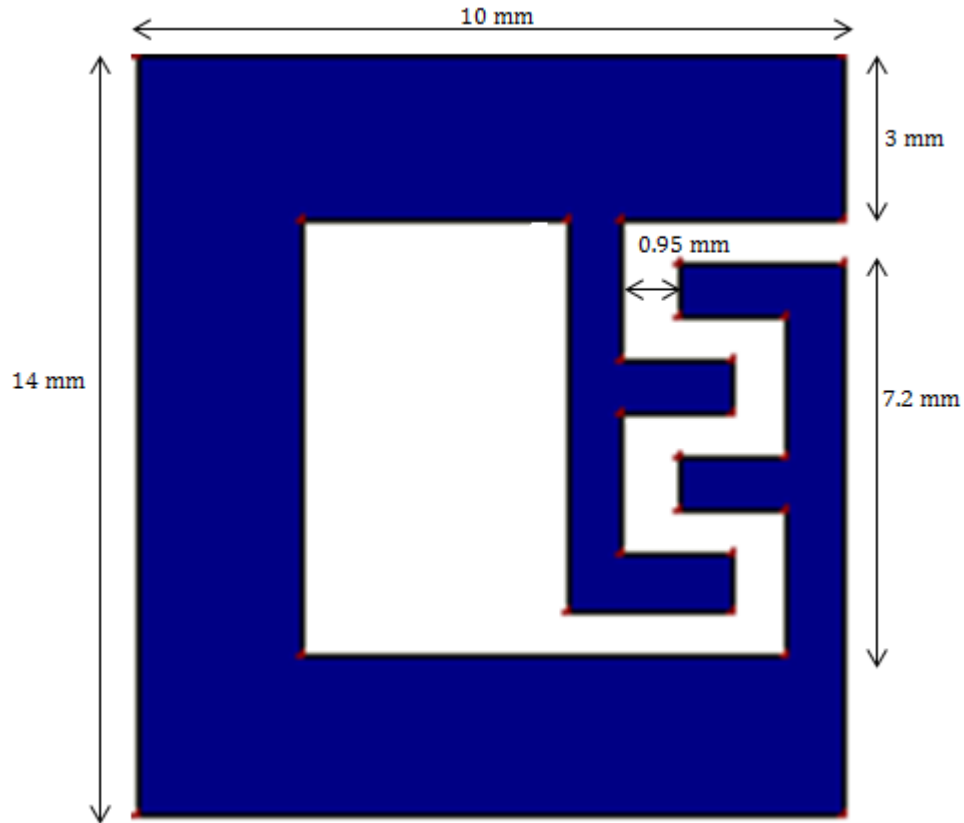


Figure 3.1: Interdigital hairpin resonator

The parameter which controls the performance of this band-pass filter is the interdigital distance of the hairpin resonator. So following our specification we changed the value of interdigital distance and observed its influence on the result and thus reached to an optimized design.

With interdigital distance 1 mm we have a BW of 250 MHz with mid-band insertion loss -0.811 dB and return loss -11.65 dB.

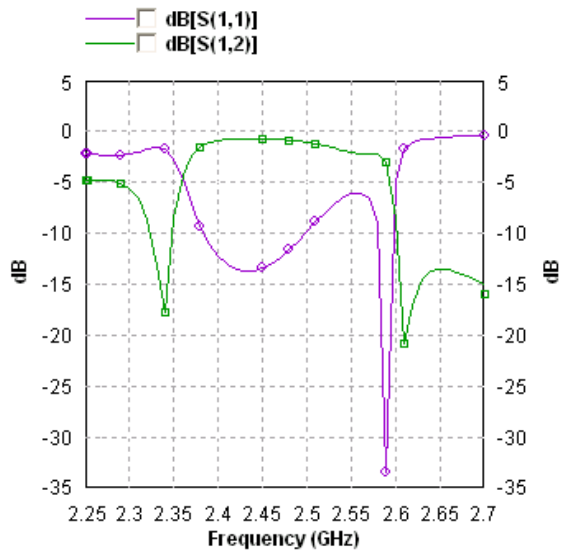


Figure 3.2: Frequency response with $I_{dd}=1$ mm

With interdigital distance 0.5 mm we have a BW of 150 MHz with mid-band insertion loss -1.02 dB and return loss -10.252 dB.

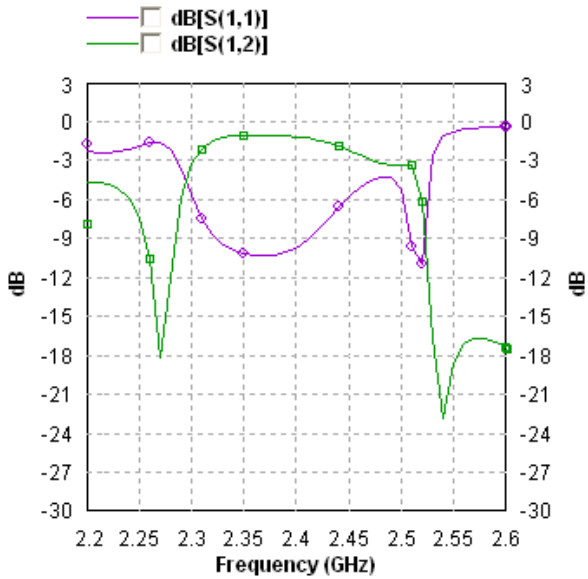


Figure 3.3: Frequency response with $I_{dd}=0.5$ mm

With interdigital distance 0.95 mm we have a BW of 220 MHz with mid-band insertion loss -0.44 dB and return loss -34.5 dB.

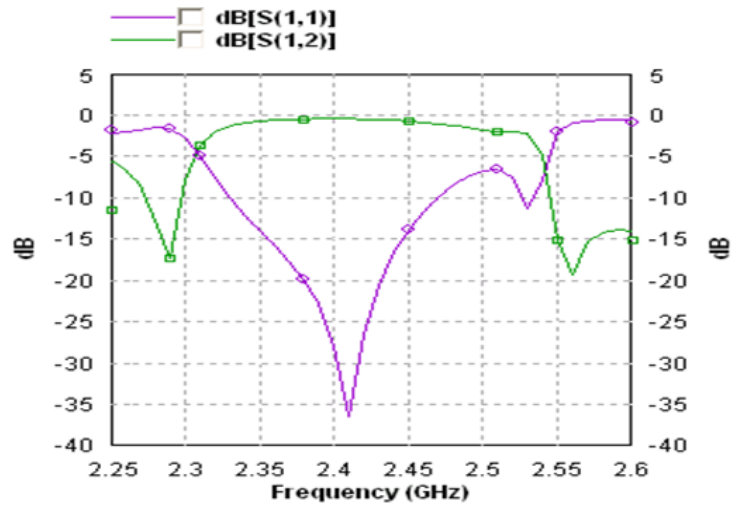


Figure 3.4: Frequency response with $I_{dd}=0.95$ mm

Figure 3.1 illustrates the hairpin resonator which we used to design our band-pass filter. Here the interdigital distance is 0.95 mm which we obtained after intensive research. Length of each hairpin is 2 mm and width is 1 mm.

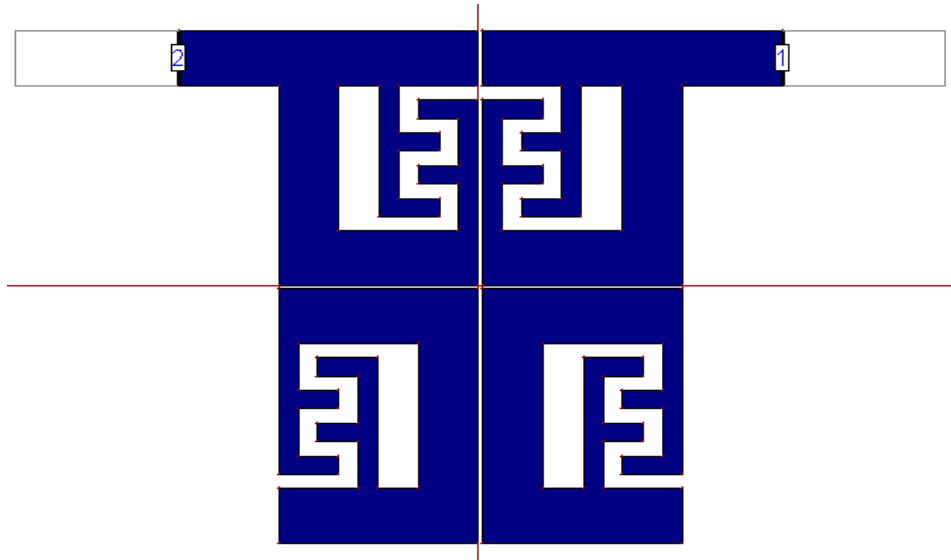


Figure 3.5: Layout of the microstrip four-pole elliptic function compact filter

Figure 3.5 illustrates the microstrip four-pole elliptic function compact filter. Distance between each pole is 0.2 mm which is also obtained through intensive research.

CHAPTER 4

Results and Simulations

4.1 Simulated result

As discussed in the previous chapter an intensive simulation has been done to optimize the filter for the frequency range of 2.31-2.53 GHz. As a result we have found a filter having area of $28.2 \times 20.2 \text{ mm}^2$.

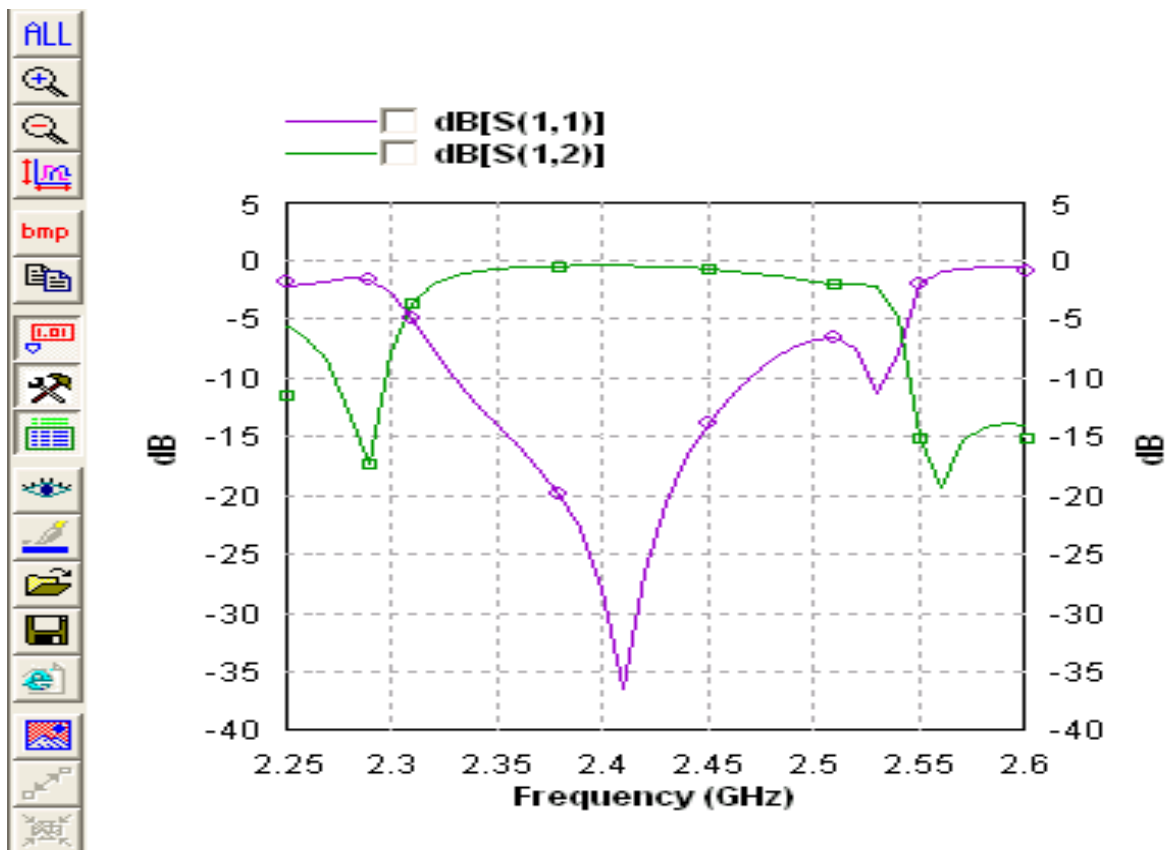


Figure 4.1: Frequency response of the proposed model

The details results obtained by simulation are:

- Lower cut-off frequency = 2.31 GHz
- Upper cut-off frequency = 2.53 GHz
- BW = 220 MHz
- $f_0 = \sqrt{f_1 \times f_2} = 2.41 \text{ GHz}$
- Return Loss at $f_0 = -34.5 \text{ dB}$
- Insertion Loss at $f_0 = -0.44 \text{ dB}$
- Percentage BW = $\text{bw} / f_0 * 100 = 9\%$
- $Q = \frac{f_0}{BW} = 11$

4.2 Comparison between existing model and our proposed model is given in the table

Table 4.1: Comparison between existing model and our proposed model:

Properties	Existing model	Proposed new model
Dimension	27.9 mm * 29.1 mm	20.2 mm * 28.2 mm
Substrate	FR4	RO4003C
Thickness	1.8 mm	1.5 mm
BW	100 MHz	220 MHz
Center frequency (f_0)	1.8GHz	2.41 GHz
PBW	5%	9%
Insertion loss at f_0	-.5 dB	-.44dB
Return loss at f_0	-25 dB	-34.5 dB

4.3 Insight into parametric study

The frequency response of the filter depends upon various parameters as earlier disused. And as a result there is a complex relationship among them. So for convenience we concentrate only on the interdigital distance.

With the variation of interdigital distance the change in the BW, frequency range, return loss, insertion loss are summarized in the next table.

Table 4.2: Parametric (Idd) study

Parameter	BW	Mid-band	Insertion loss	Return loss
Idd=1 mm	250 MHz	2.47 GHz	-0.811 dB	-11.65 dB
Idd=0.95	220 MHz	2.41 GHz	-0.44 dB	-34.5 dB
Idd=0.5 mm	150 MHz	2.37 GHz	-1.02 dB	-10.252 dB

So with the decrease of interdigital distance BW decreases and mid-band frequency also decreases. But in the case of return loss and insertion loss when interdigital distance is less than 0.95 mm there is some irregularities and the filter response becomes poor.

CHAPTER 5

Conclusion

In this thesis a four pole microstrip band-pass filter is designed and optimized for the frequency range of 2.31-2.53 GHz. The filter showed satisfactory simulation result. The proposed filter showed improvement in terms of BW, return loss, quality factor, size, fractional BW from any existing filter in this band. A reduction in the filter area has been achieved as our proposed filter only requires the area of $28.2*20.2 \text{ mm}^2$ which is smaller than the area of the filter found in the literature review. The result of the parametric study is summarized in the table which can be used for further study in this field.

All the optimization has been achieved using Zeland's IE3D electromagnetic simulator. This filter can be fabricated in real time and further study can be done to increase the BW and reduce the return loss.

S Parameters

For a generic multi-port network, each of the ports is allocated an integer 'n' ranging from 1 to N, where N is the total number of ports. For port n, the associated S-parameter definition is in terms of incident and reflected 'power waves', a_n and b_n respectively.

Two-port S parameters

The S-parameter matrix for the 2-port network is probably the most commonly used and serves as the basic building block for generating the higher order matrices for larger networks. In this case the relationship between the reflected, incident power waves and the S-parameter matrix is given by



$$\begin{pmatrix} b_1 \\ b_2 \end{pmatrix} = \begin{pmatrix} s_{11} & s_{12} \\ s_{21} & s_{22} \end{pmatrix} \begin{pmatrix} a_1 \\ a_2 \end{pmatrix}$$

Expanding the matrices into equations gives:

$$b_1 = s_{11}a_1 + s_{12}a_2$$

And

$$b_2 = s_{21}a_1 + s_{22}a_2$$

Each equation gives the relationship between the reflected and incident power waves at each of the network ports, 1 and 2, in terms of the network's individual S-parameters, s_{11} , s_{12} , s_{21} and s_{22} . If one considers an incident power wave at port 1 (a_1) there may result from it waves exiting from either port 1 itself (b_1) or port 2 (b_2). However if, according to the definition of S-parameters, port 2 is terminated in a load identical to the system impedance (Z_0) then, by the maximum power transfer theorem, b_2 will be totally absorbed making a_2 equal to zero. Therefore

$$S_{11} = \frac{b_1}{a_1}$$

$$S_{12} = \frac{b_1}{a_2}$$

$$S_{21} = \frac{b_2}{a_1}$$

$$S_{22} = \frac{b_2}{a_2}$$

Each 2-port S-parameter has the following generic descriptions:

S_{11} is the input port voltage reflection coefficient

S_{12} is the reverse voltage gain

S_{21} is the forward voltage gain

S_{22} is the output port voltage reflection coefficient

S-Parameter properties of 2-port networks

An amplifier operating under linear (small signal) conditions is a good example of a non-reciprocal network and a matched attenuator is an example of a reciprocal network. In the following cases we will assume that the input and output connections are to ports 1 and 2 respectively which is the most common convention. The nominal system impedance, frequency and any other factors which may influence the device, such as temperature, must also be specified.

Insertion loss

Input return loss (RL_{in}) is a scalar measure of how close the actual input impedance of the network is to the nominal system impedance value and, expressed in logarithmic magnitude, is given by

$$RL_{in} = |20 \log_{10} |S_{11}| | \text{ dB}$$

By definition, return loss is a positive scalar quantity implying the 2 pairs of magnitude (|) symbols. The linear part, $|S_{11}|$ is equivalent to the reflected voltage magnitude divided by the incident voltage magnitude.

Output return loss

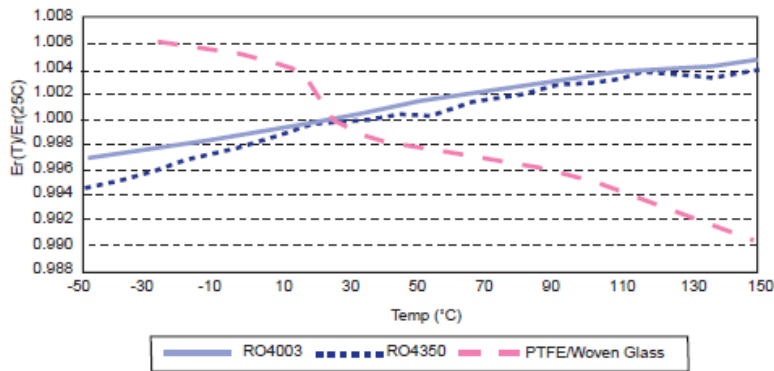
The output return loss (RL_{out}) has a similar definition to the input return loss but applies to the output port (port 2) instead of the input port. It is given by

$$RL_{out} = |20 \log_{10} |S_{22}| | \text{ dB}$$

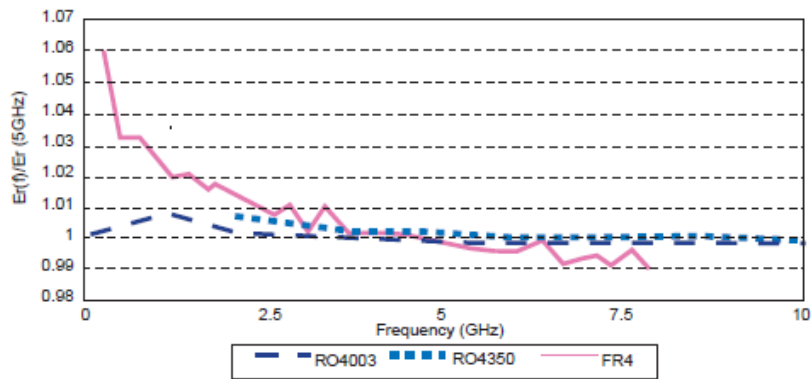
Table A1: RO4000® Series Laminate Product Information

PROPERTY	TYPICAL VALUES		DIRECTION	UNITS	CONDITION	TEST METHOD
	RO4003 ^(a)	RO4350B ^(b)				
Dielectric Constant ϵ_r	3.38 ± 0.05	3.48 ± 0.05	Z	-	10 GHz/23°C	IPC-TM-650 2.5.5.5
Dissipation Factor, tan (δ)	0.0027	0.0040	Z	-	10 GHz/23°C	IPC-TM-650 2.5.5.5
Thermal Coefficient of ϵ_r	+40	+50	Z	ppm°C	-100°C to 250°C	IPC-TM-650 2.5.5.5
Volume Resistivity	1.7 x 10 ¹⁰	1.2 x 10 ¹⁰	-	MΩ	COND A	IPC-TM-650 2.5.17.1
Surface Resistivity	4.2 x 10 ⁹	5.7 x 10 ⁹	-	MΩ	COND A	IPC-TM-650 2.5.17.1
Electrical Strength	25.6 (650)	31.5 (800)	Z	KV/mm (V/mil)	0.51mm (0.020")	IPC-TM-650 2.5.6.2
Tensile Modulus	26,889 (3900)	11,473 (1664)	Y	MPa (kpsi)	RT	ASTM D638
Tensile Strength	141 (20.4)	175 (25.4)	Y	MPa (kpsi)	RT	ASTM D638
Flexural Strength	276 (40)	255 (37)	-	MPa (kpsi)	-	IPC-TM-650 2.4.4.
Dimensional Stability	<0.3	<0.5	X,Y	mm/m (mils/inch)	After etch +E2/150	IPC-TM-650 2.2.4
Coefficient of Thermal Expansion	11 14 46	14 16 50	X Y Z	ppm°C	-55 to 288°C	IPC-TM-650 2.1.4.1
Tg	>280	>280	-	°C	2.4.24	TMA
Thermal Conductivity	0.64	0.62	-	W/m*K	100°C	ASTM F433
Specific Gravity	1.79	1.86	-	-	23°C	ASTM D792
Water Absorption	0.04	0.02	-	%	48 hrs. Immersion 0.060" sample Temperature 50°C	ASTM D570
Copper Peel Strength	1.05 (6.0)	0.88 (5.0)	-	N/mm (pli)	after solder float	IPC-TM-650 2.48
Flammability	N/A	UL 94V-O	-	-	-	

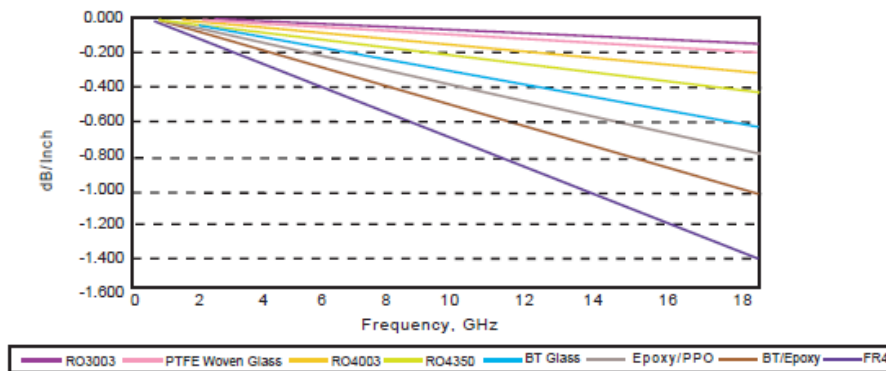
**Table A2: RO4000 Series Materials
Dielectric Constant vs. Temperature**



**Table A3: RO4000 Series Materials
Dielectric Constant vs. Frequency**



**Table A4: Microstrip Insertion Loss
(0.030" Dielectric Thickness)**



APPENDIX B

- [1] Run Zeland Program Manager. You will see a layout similar to that shown in Figure B1

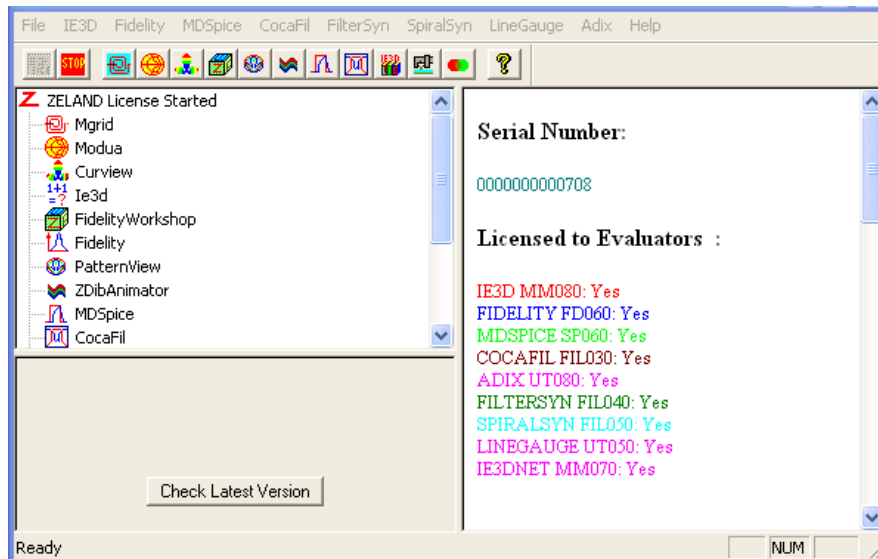

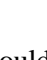


Figure B1: Zeland Program Manager

- [2] Run MGRID by clicking on the MGRID button () shown in Figure B1. MGRID is the main interface of IE3D, in which you can draw the layout of the circuit to be simulated.
- [3] Click the new button as shown in Figure B2 () .
- [4] The basic parameter definition window pops up. You should see something similar to Figure B3. In this window you can define basic parameters of the simulation such as the dielectric constant of different layers, the units and layout dimensions, and metal types among other parameters. In “Substrate Layer” section note that two layers are automatically defined. At $z=0$, the program automatically places an infinite ground plane (note the material conductivity at $z=0$) and a second layer is defined at infinity with the dielectric constant of 1.

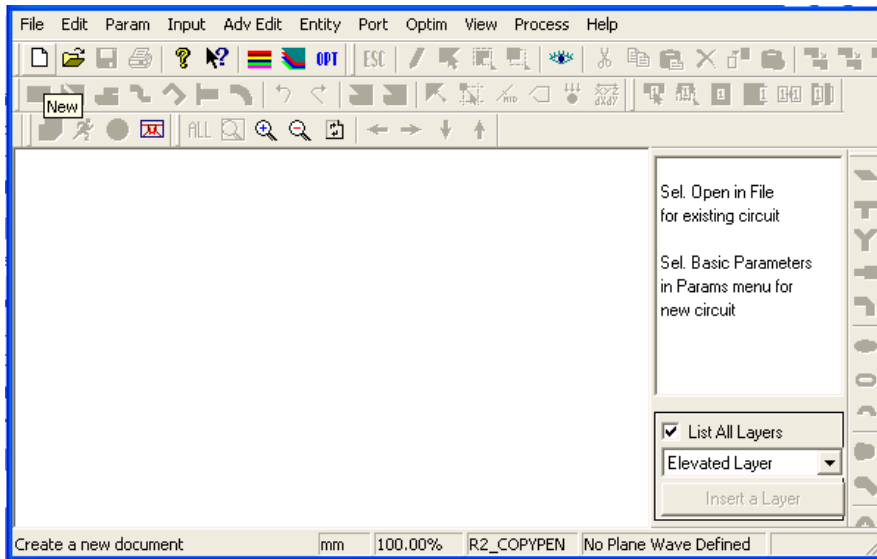


Figure B2: Main view of MGRID

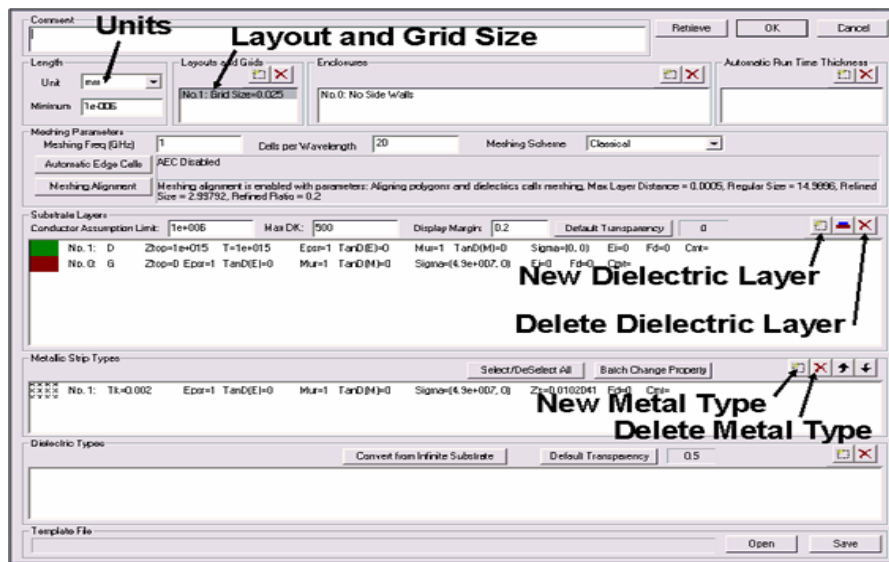



Figure B3: Basic parameter definitions

- [5] In the basic parameter definition window, click on “New Dielectric Layer” button () as is shown in Figure B3. You will see a window similar to the one shown in Figure B4. Enter the basic dielectric parameters in this window:

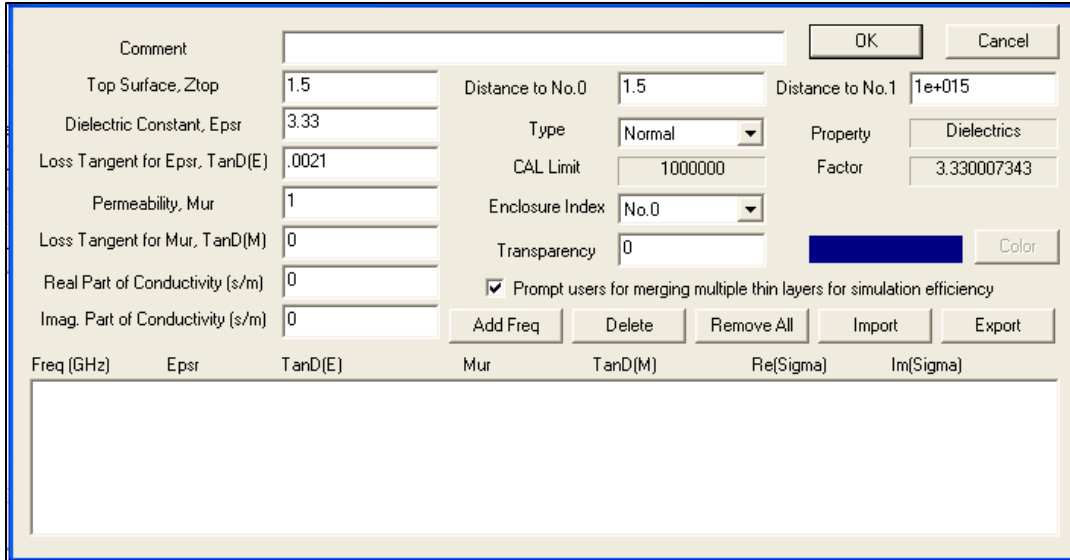


Figure B4: Defining the parameters of the filter substrate

- a. Top surface, Z_{top} : Enter the z dimension of the top surface. In this case, it is 1.5 mm
- b. Dielectric Constant: This field represents the dielectric constant of the layer. Enter 3.3 here for the dielectric constant of the RO4003C substrate
- c. Loss tangent: Enter 0.0021 for the loss tangent in this field.

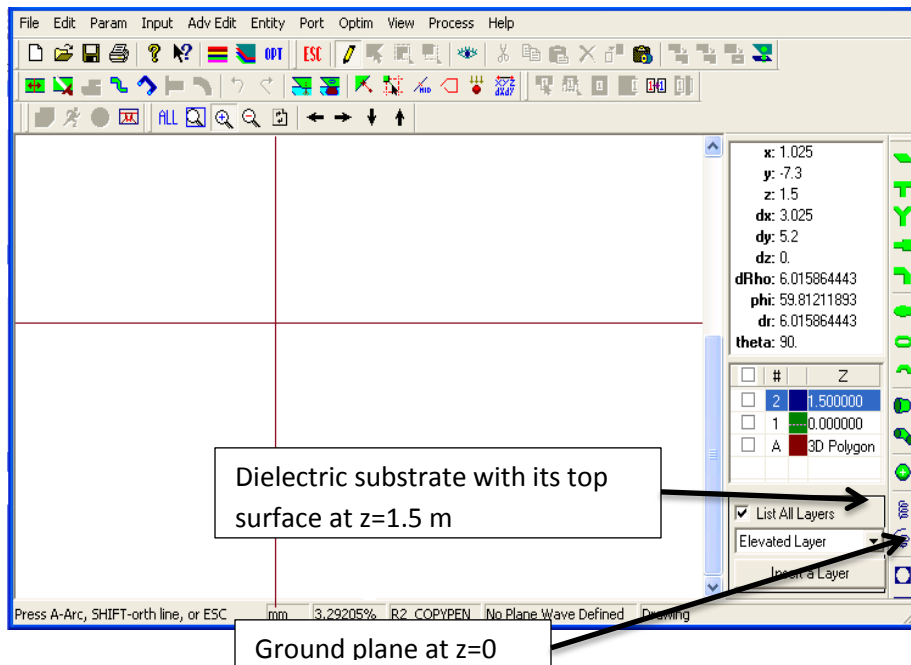



Figure B5: Layout view of the problem after the definition of the dielectric layers

[6] The next step is to draw the filter and the layout. In this case we will use a rectangular patch, fed with a simple microstrip line. The feeding microstrip line is a 50Ω line and the impedance of the

filter is matched to 50Ω by using an inset feed. We will draw the structure in multiple stages as follows in the following steps.

- [7] First, we will draw a rectangle with the length of 10 mm and width of 3 mm. Click on the rectangle script button shown in Figure B6 (). Enter 12 for Length and 3 for width as shown in Figure B6 and click OK. Now your layout should look like Figure B7.

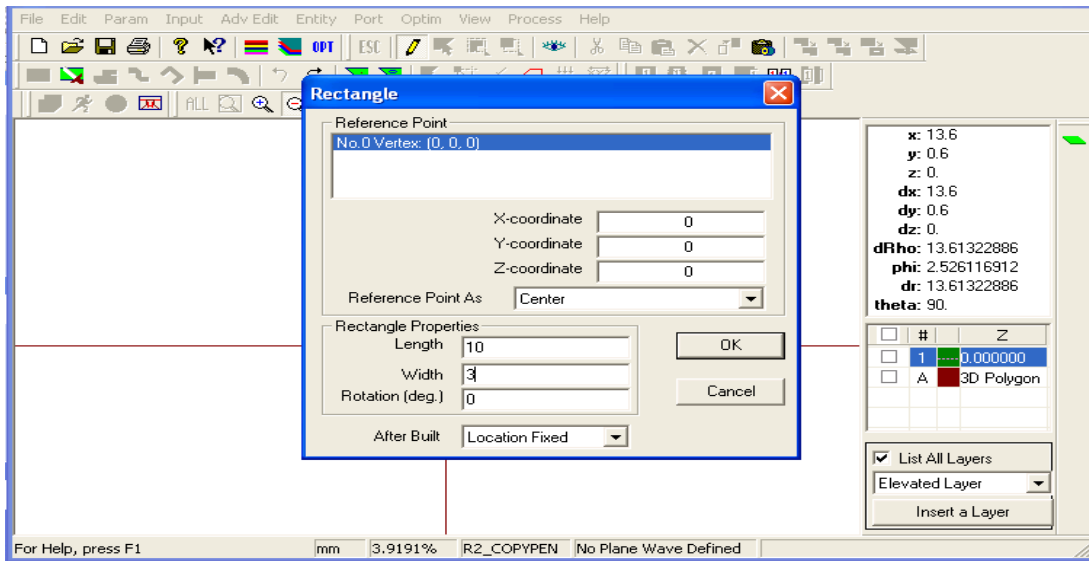


Figure B6: Rectangle pop-up window

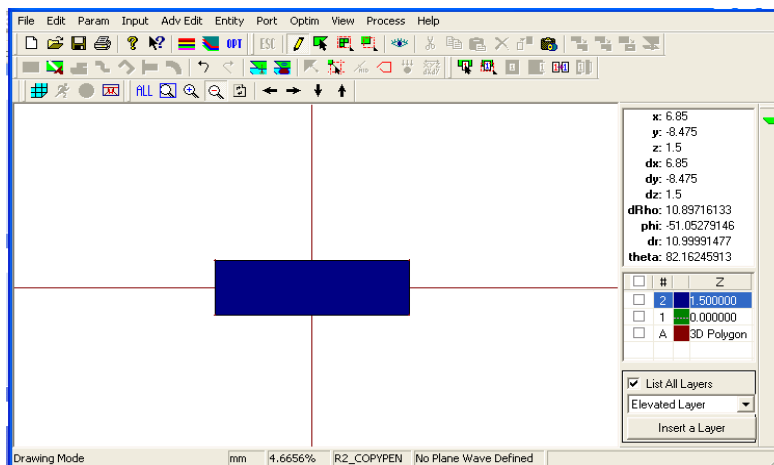


Figure B7: Mgrid window

The next step is to draw the rest of the structure. Press Shift+A. The “Keyboard Input Absolute Location” menu pops up. In this menu, you can place a vertex at an arbitrary location on the layout. Enter -5 for x and -1.5 for y values. Your screen should look like Figure B8. Click on OK button. The “Close Vertices” menu pops up. Click on YES to adjust this vertex to be connected to the one at (-5mm, -1.5 mm). This vertex will then be connected to the one on the lower left corner of the rectangle drawn in the previous step

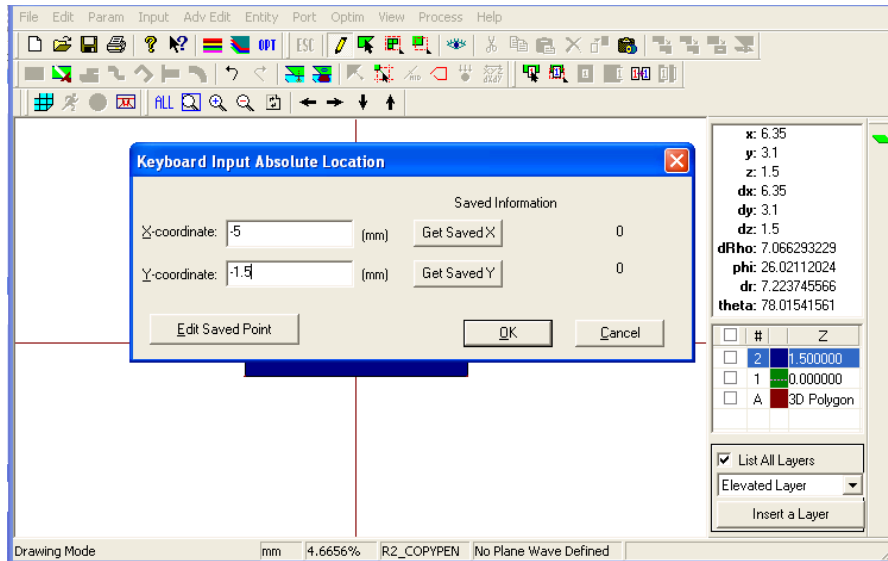


Figure B8: Keyboard input absolute input location pop-up window

- [9] Press Shift+R. The “Keyboard Input Relative Location” menu pops up. Now that you have entered the absolute location of the first vertex, you can use that as a reference point and enter the location of additional vertices relative to the one entered previously. Enter 0 for the X-offset and -11 for the Y-offset values. Your screen should look like the one shown in Figure B9. Click on OK button and Click on YES button in the next menu that pops up.

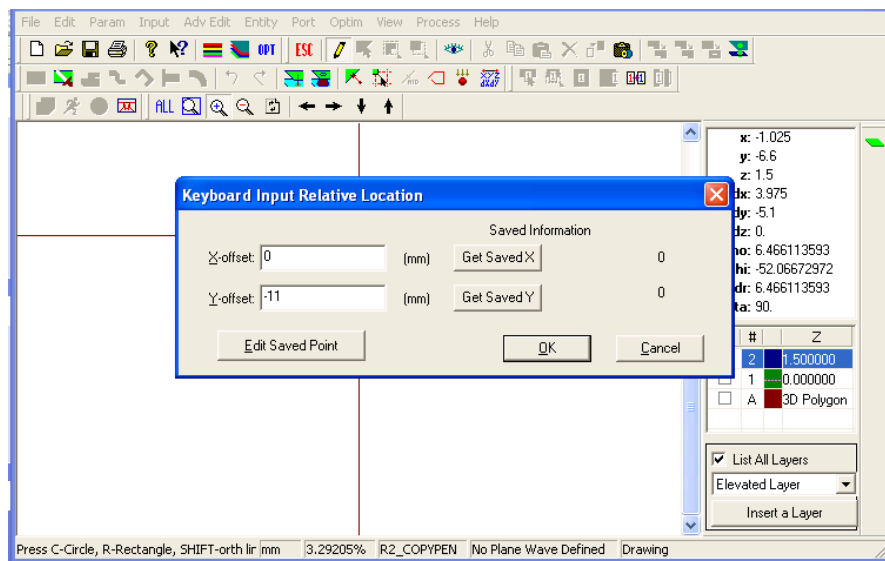


Figure B9: Keyboard input relative location pop-up window

- [10] Press Shift+R again and Enter 3 for the X-offset and 0 for the Y-offset values. Press OK.
- [11] Press Shift+F. This short cut creates a rectangle using the three vertices that are entered already. Your screen should look like Figure B10 at this stage.

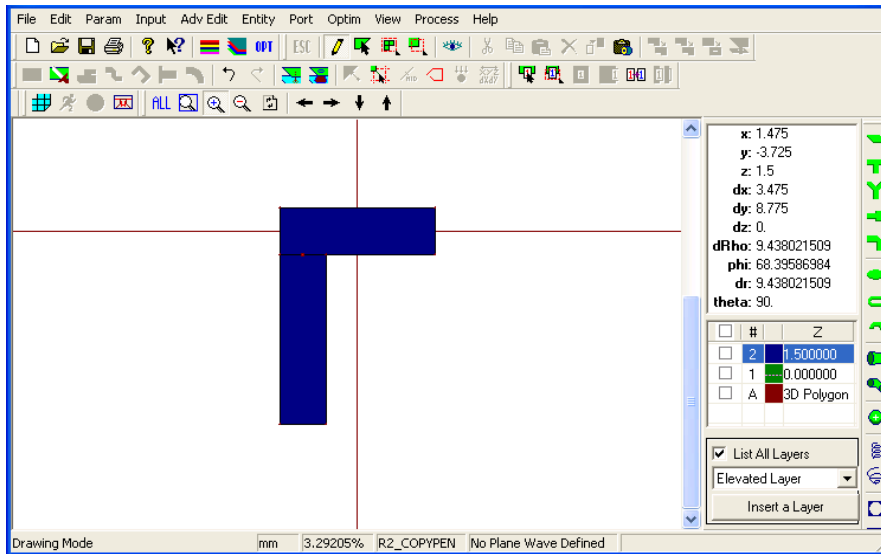


Figure B10: Mgrid window

- [12] Press Shift+A. Enter -2 for x and -12.5 for y values. Click on OK button. Then click on YES
- [13] Press Shift+R. Enter 7 for the X-offset and 0 for the Y-offset values. Press OK.
- [14] Press Shift+R. Enter 0 for the X-offset and 3 for the Y-offset values. Press OK.
- [15] Press Shift+F. This short cut creates a rectangle using the three vertices that are entered already. Your screen should look like Figure B11 at this stage.

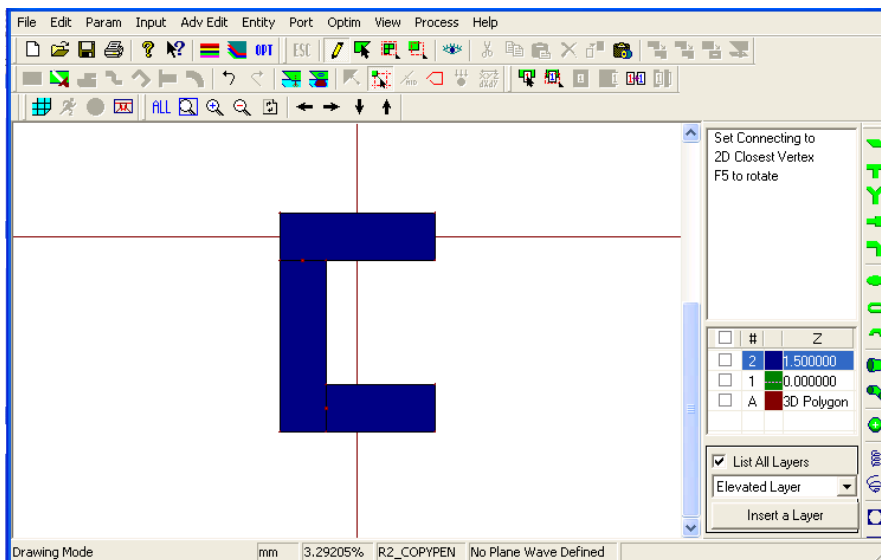


Figure B11: Mgrid window

- [16] Press Shift+A. Enter 5 for x and -9.5 for y values. Press OK
- [17] Press Shift+R. Enter 0 for the X-offset and -7.2 for the Y-offset values. Press OK

- [18] Press Shift+R . Enter -1 for the X-offset and 0 for the Y-offset values. Press OK.19. Press Shift+F. This short cut creates a rectangle using the three vertices that are entered already. Your screen should look like Figure B12 at this stage.

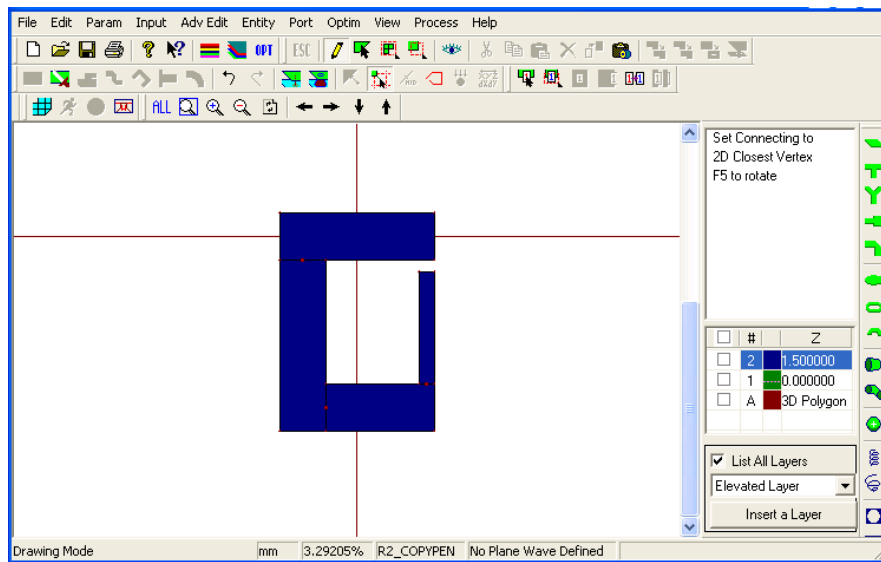


Figure B12: Mgrid window

- [20] Press Shift+A. Enter 4 for x and -2.3 for y values. Press OK
 [21] Press Shift+R. Enter -2 for the X-offset and 0 for the Y-offset values. Press OK
 [22] Press Shift+R again and Enter 0 for the X-offset and -1 for the Y-offset values. Press OK.
 [23] Press Shift+F. This short cut creates a rectangle using the three vertices that are entered already. Your screen should look like Figure B13 at this stage.

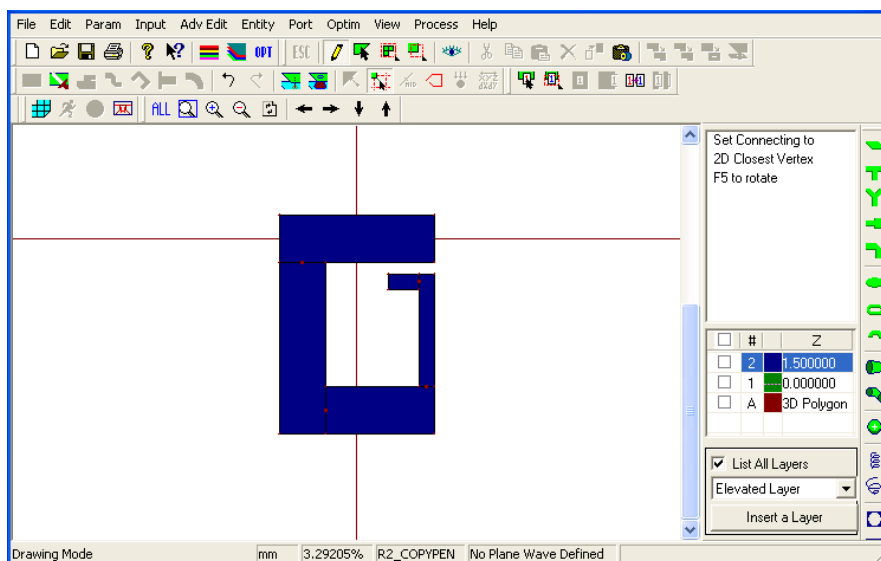


Figure B13: Mgrid window

- [24] Press Shift+A. Enter 4 for x and -6 for y values. Click on OK button.
 [25] Press Shift+R. Enter -2 for the X-offset and 0 for the Y-offset values. Press OK
 [26] Press Shift+R again and Enter 0 for the X-offset and -1 for the Y-offset values. Press OK

- [27] Press Shift+F. This short cut creates a rectangle using the three vertices that are entered already. Your screen should look like Figure B14 at this stage.

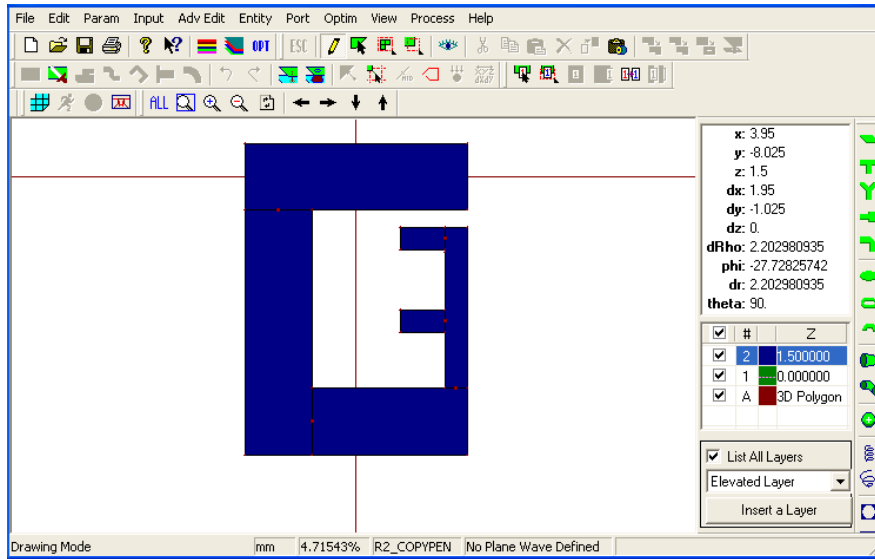


Figure B14: Mgrid window

- [28] Press Shift+A. Enter -.05 for x and -1.5 for y values. Press OK
[29] Press Shift+R. Enter 0 for the X-offset and -7.2 for the Y-offset values. Press OK.
[30] Press Shift+R again and Enter 1 for the X-offset and 0 for the Y-offset values. Press OK.
[31] Press Shift+F. This short cut creates a rectangle using the three vertices that are entered already. Your screen should look like Figure B15 at this stage.

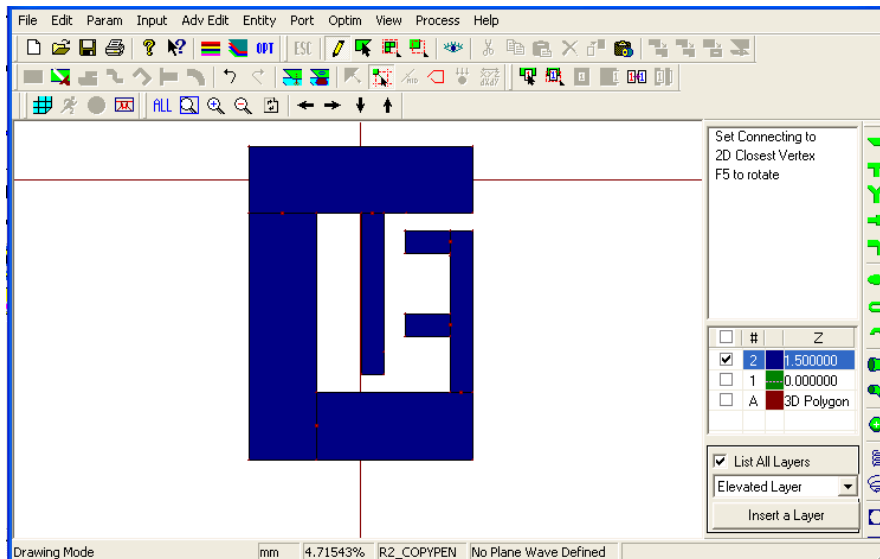


Figure B15: Mgrid window

- [32] Press Shift+A. Enter 1.05 for x and -8.7for y values. Press OK
[33] Press Shift+R. Enter 2 for the X-offset and 0 for the Y-offset values. Press OK

- [34] Press Shift+R again and Enter 0 for the X-offset and 1 for the Y-offset values. Press OK. 35. Press Shift+F. This short cut creates a rectangle using the three vertices that are entered already. Your screen should look like Figure B16 at this stage.

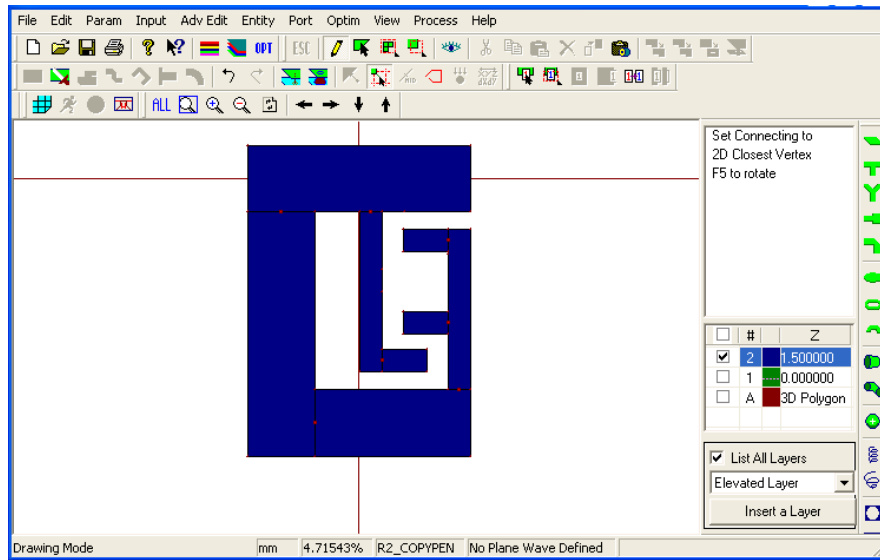


Figure B16: Mgrid window

- [36] Press Shift+A. Enter 1.05 for x and -5.1 for y values. Press OK
 [37] Press Shift+R. Enter 2 for the X-offset and 0 for the Y-offset values. Press OK
 [38] Press Shift+R again and Enter 0 for the X-offset and 1 for the Y-offset values. Press OK.
 [39] Press Shift+F. This short cut creates a rectangle using the three vertices that are entered already. Your screen should look like Figure B17 at this stage.

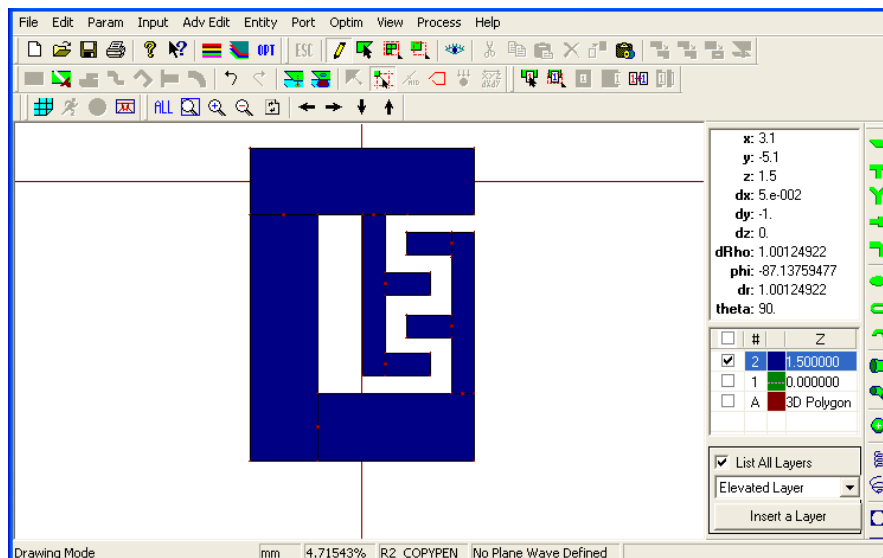




Figure B17: Mgrid window

- [40] Click the select polygon as shown in Figure B18 (). The shape of mouse cursor changes from the cross “+” to the ordinary mouse cursor ().

- [41] Move the mouse cursor on a blank spot and click on it and make a rectangle with it . It will be highlighted in black as shown in figure B18

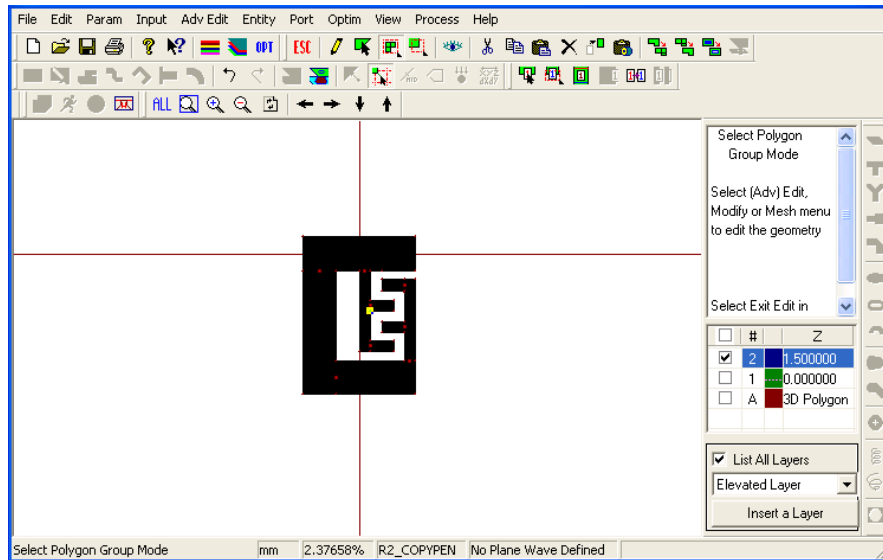


Figure B18: Mgrid window

- [42] Click “Edit” then select “Move object” or Press Shift+M. Place the structure at any place and move object original to offset window pops up. Enter for X-offset and -5.1 for Y-offset values

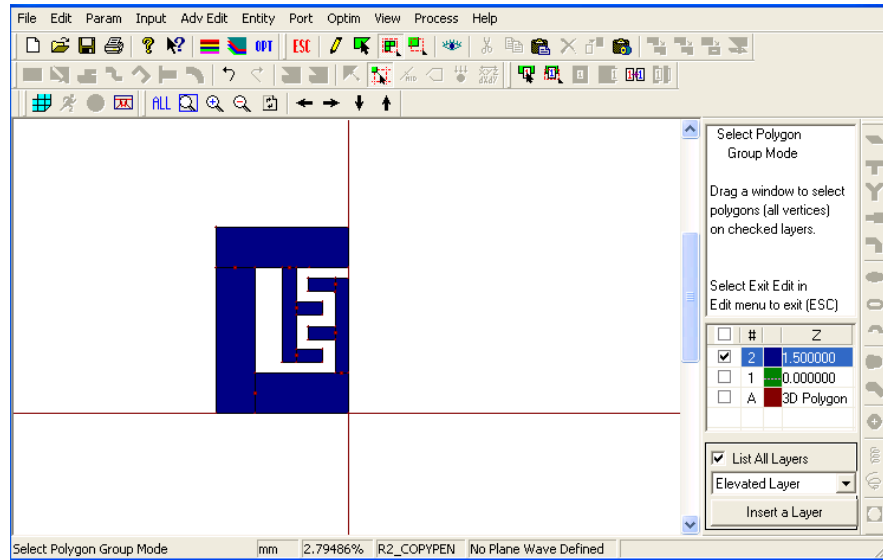



Figure B19: Mgrid window

- [43] Click the select polygon (). Select the whole structure. Click “Edit” then select “Copy and reflect”. Then reflection angle menu pops up. Give object reflection angle 0 then press OK. After that copy and reflect objects window pops up. Give minimum reflection distance .2 mm then press OK. You will get a figure in your screen as shown in figure B20.

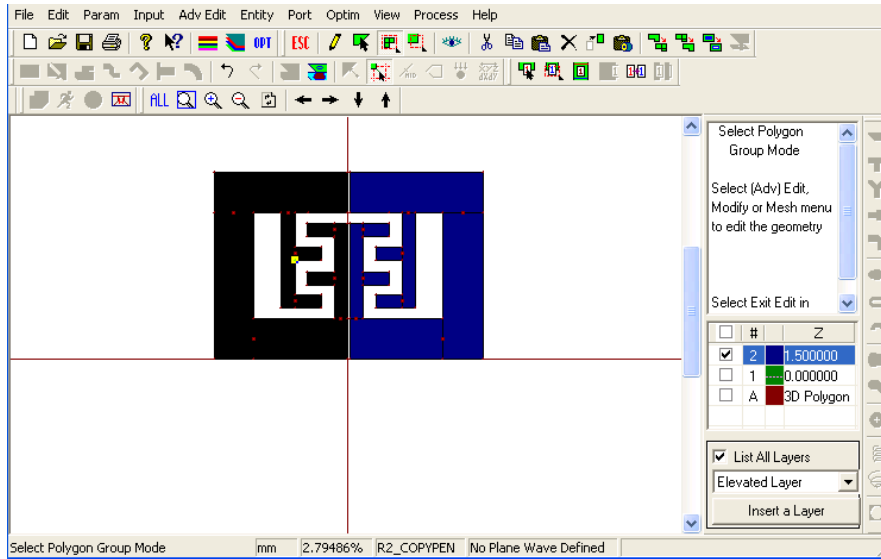


Figure B20: Mgrid window

[44] Press Ctrl+C. Then press Shift+C and place the copied object in the place as shown in figure B21

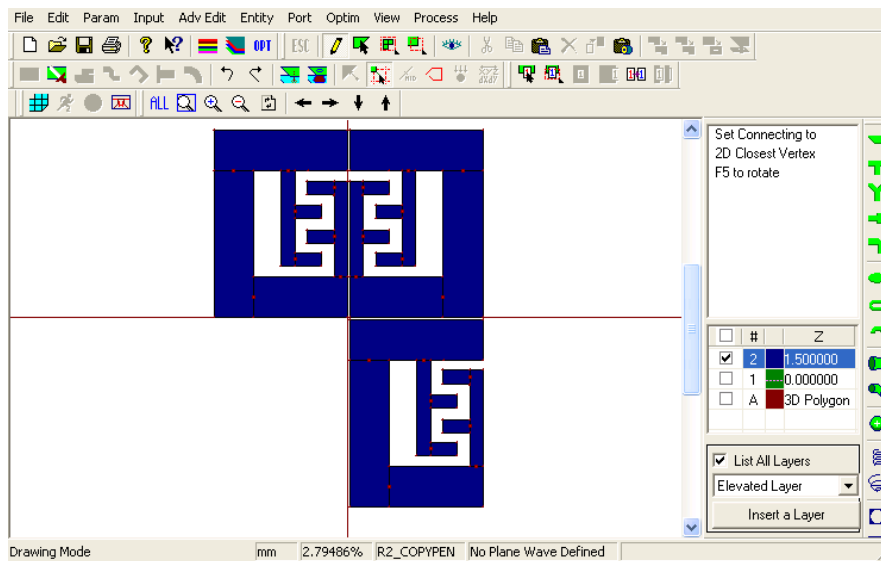



Figure B21: Mgrid window

[45] Click the select polygon (). Select the lower part of the total structure. Click “Edit” then select “Copy and reflect”. Then reflection angle menu pops up. Give object reflection angle 180 then press OK. After that copy and reflect objects window pops up. Give minimum reflection distance 0.2 mm then press OK. You will get a figure in your screen as shown in figure B22.

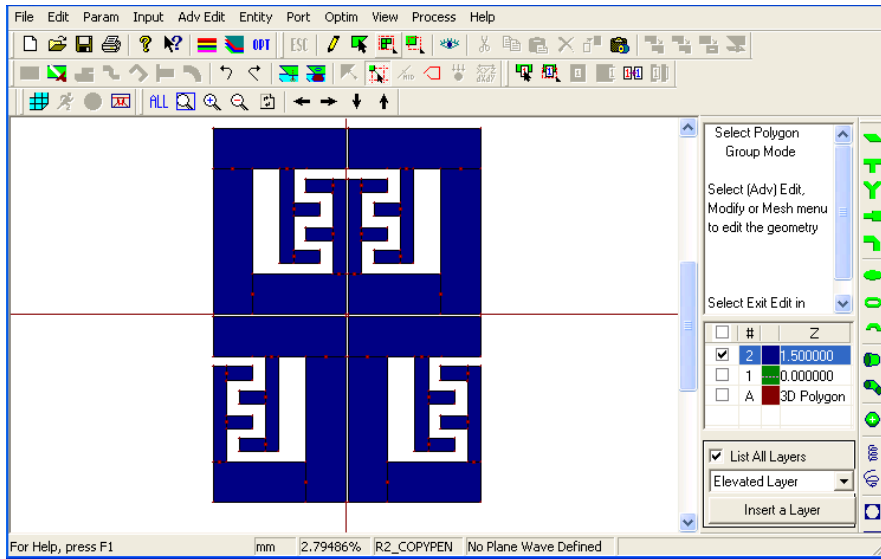



Figure B22: Mgrid window

- [46] Press Shift+A. Enter 10.2 for x and 14 for y values. Press OK
- [47] Press Shift+R. Enter 3 for the X-offset and 0 for the Y-offset values. Press OK
- [48] Press Shift+R again and Enter 0 for the X-offset and -3 for the Y-offset values. Press OK.
- [49] Press Shift+F
- [50] Press Shift+A. Enter -10 for x and -14 for y values. Click on OK button.
- [51] Press Shift+R. Enter -3 for the X-offset and 0 for the Y-offset values. Press OK
- [52] Press Shift+R again and Enter 0 for the X-offset and -3 for the Y-offset values. Press OK.
- [53] Press Shift+F.
- [54] The next stage is to setup excitation. We are going to use a port to excite the microstrip line, which in turn feeds the patch.
- [55] Click the “define port” () button. Then “De-Embedding scheme” window pops up. Select “Advanced extension” and Leave the rest of the fields unchanged at this stage and press the OK button. Then place the ports at the two ends of the extension of the structure shown at figure B23

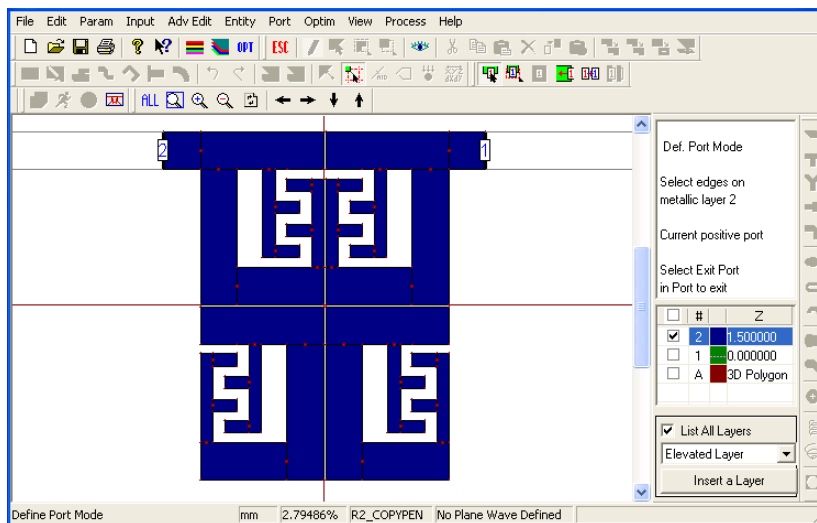



Figure B23: Mgrid window

- [56] Click the select polygon (). Select the whole structure. Click “Adv edit” then select “Merge Selected Polygons”. Then press OK. The structure will be like one as shown in the figure B24

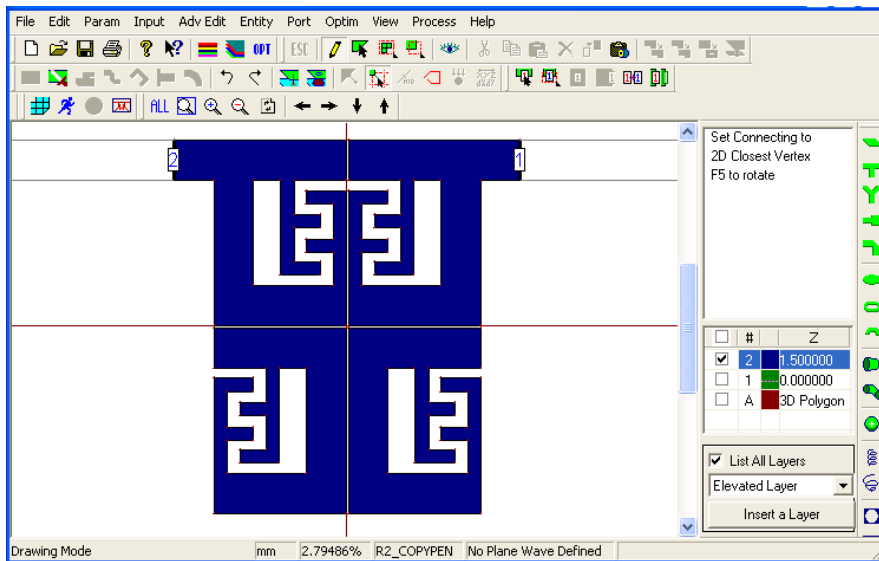



Figure B24: Mgrid window

- [57] The next step is to run the simulation. However, before that, let us first mesh the structure; this mesh is used in the Method of Moment (MoM) calculation. Press the “Display Meshing” button (). The “Automatic Meshing Parameters” menu pops up. This menu is shown in Figure B25.

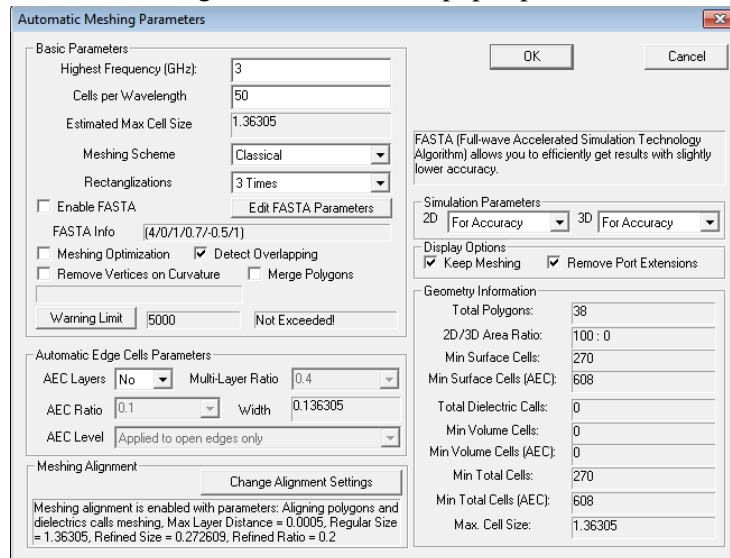


Figure B25: Automatic meshing parameter pop-up window

- [58] In this menu, you have to specify the highest frequency that the structure will be simulated at. Enter 3 in the “Highest Frequency” field. In this case, the operating frequency is 2.4 GHz. Therefore choosing 3 GHz as the maximum frequency should be OK. Enter 50 in the “Cells per Wavelength” field. The number of cells/wavelength determines the density of the mesh. In

method of moment simulations, you should not use fewer than 10 cells per wavelength. The higher the number of cells per wavelength, the higher the accuracy of the simulation. However, increasing the number of cells increases the total simulation time and the memory required for simulating the structure.

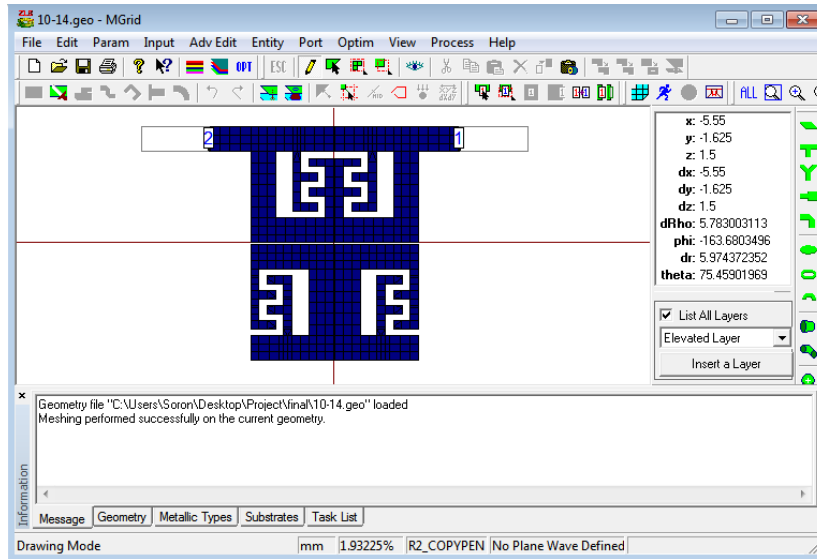



Figure B26: Mgrid window

- [59] Note that in meshing this structure, we did not use edge cells. As seen in Figure B25, in the “Automatic Edge Cell Parameters” fields, the “AEC Layers” field shows “NO”. You can define edge cells to increase the accuracy of the simulations. In coupled structures or in structures where multiple trace lines are located in close proximity to each other, it is important to use edge cells. In this case, we will not use edge cells for this simulation.
- [60] Now it is time to simulate the structure. Press the “Run Simulation” button (). The simulation setup window pops up. Here you can specify the simulation frequency points as well as the basic parameters of the mesh. Click on Enter button in the Frequency parameters field. Enter 1 in the “Start Freq (GHz)” field, 3 at the “End Freq (GHz)” field, and 201 in the “Number of Freq” field and click OK. The “Frequency Parameters” field is now filled with 201 evenly spaced frequency points between 1 GHz and 3 GHz range. Make sure that the “Adaptive Intelli-Fit” check box is checked as shown in Figure 22. When Adaptive Intelli-Fit is enabled, the program does not perform simulations at all of the specified frequency points. It automatically selects a number of frequency points and simulates the structure at these particular points and interpolates the response based on the simulated points. Depending on the number of resonances and the Q of the structure at each resonance, IE3D determines the number of frequency points that the actual simulation is performed at.

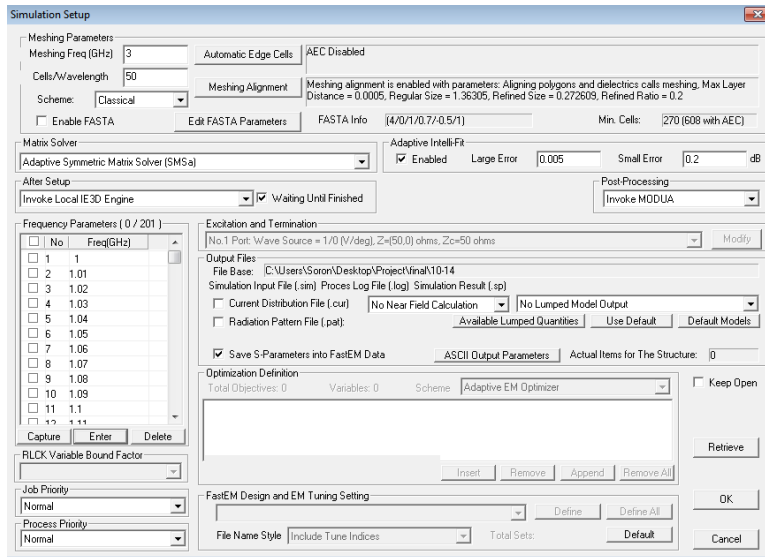


Figure B27: Simulation setup pop-up window

- [61] Press OK and the structure will be simulated. The simulation progress window shows the progress of the simulation. It will only take a couple of seconds for the simulation to finish. After the simulation is completed, IE3D automatically invoked MODUA and shows the S parameters of the simulated structure.

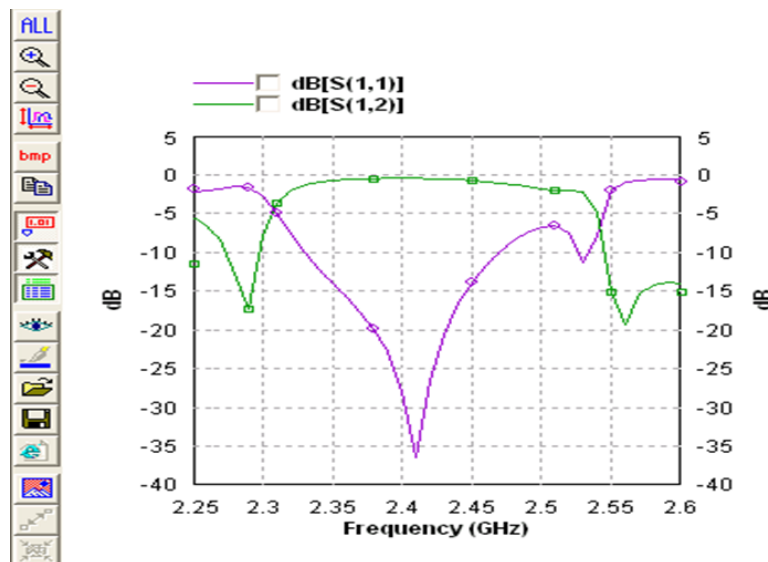


Figure B28: Frequency response in Modua

- [62] In MODUA, you can examine the frequency response of the circuit in different formats. Press Ctrl+G and the “Display Parameters” window pops up. You can select the Z parameters, Y parameters, S parameters, etc.

REFERENCES

- [1] S.B. Cohn, Parallel-coupled transmission line resonator filters, *IRE Trans Microwave Theory Tech* 6 (1958), 223–231.
- [2] S. Caspi and J. Adelman, Design of combline and interdigital filter with tapped-line input, *IEEE Trans Microwave Theory Tech* 36 (1988), 759–763.
- [3] G.L. Matthaei, Comb-line bandpass filter of narrow or moderate bandwidth, *IEEE Trans Microwave Theory Tech* 6 (1963), 82–91.
- [4] U.H. Gysel, New theory and design for hairpin-line filters, *IEEE Trans Microwave Theory Tech* 22 (1974), 523–531.
- [5] E.G. Cristal and S. Frankel, Hairpin-line and hybrid hairpin-line/halfwave parallel-coupled-line filters, *IEEE Trans Microwave Theory Tech* 20 (1972), 719–728.
- [6] J.S. Hong and M.J. Lancaster, Cross-coupled microstrip hairpin-resonator filters, *IEEE Trans Microwave Theory Tech* 46 (1998), 118–122.
- [7] G.L. Matthaei, N.O. Fenzi, R.J. Forse, and S.M. Rohlfing, Hairpincomb filters for HTS and other narrow-band applications, *IEEE Trans Microwave Theory Tech* 45 (1997), 1226–1231.
- [8] M. Sagawa, K. Takahashi, and M. Makimoto, Miniaturized hairpin resonator filters and their application to receiver front-end MIC's, *IEEE Trans Microwave Theory Tech* 37 (1989), 1991–1997.
- [9] H. Yabuki, M. Sagawa, and M. Makimoto, Voltage controlled pushpush oscillators using miniaturized hairpin resonators, *IEEE MTT-S Int Microwave Symp Dig*, Boston, MA (1991), 1175–1178.
- [10] R. Levy, Filters with single transmission zeros at real or imaginary frequencies, *IEEE Trans Microwave Theory Tech* 24 (1976), 172–181.
- [11] R.M. Kurzok, General four-resonator filters at microwave frequencies, *IEEE Trans Microwave Theory Tech* 14 (1966), 295–296.
- [12] S.Y. Lee and C.M. Tsai, New cross-coupled filter design using improved hairpin resonators, *IEEE Trans Microwave Theory Tech* 48 (2000), 2482–2490.
- [13] H. Yabuki, Y. Endo, M. Sagawa, and M. Makimoto, Miniaturized hairpin resonators and their application to push-push oscillators, *Proceedings of The 3rd Asia-Pacific Microwave Conference*, Tokyo, Japan, 1990, pp. 263–266.
- [14] J.S. Hong and M.J. Lancaster, *Microstrip filters for RF/Microwave applications*, Wiley, New York, 2001.
- [15] Zeland Software, *IE3D 6.0*, Zeland Software, Inc., New York, 1999.
- [16] www.apcircuits.com/resources/information/ro4000ds_4.pdf